PhD
Program in Translational
and Molecular Medicine
DIMET

University of Milano-Bicocca
School of Medicine and Faculty of Science

Tumour-released Liver X Receptor ligands attract tumour promoting neutrophils in a CXCR2 dependent manner

Coordinator: Prof. Andrea Biondi
Tutor: Prof.Francesca Granucci
Co-tutor: Dr. Vincenzo Russo

Dr.Raccosta Laura
Matr. No. 725245

XXIV CYCLE
ACADEMIC YEAR
2010-2011

The research presented in this thesis was performed at H.S Raffaele at the department of Cancer Gene Therapy Unit Program in Immunology, Immunobiotherapy and Gene Therapy of Cancer, headed by Dr. Vincenzo Russo.

Table of content

Chapter 1

1.1 Tumor and immunity

Tumours can be considered like new organs that are made of various cell types and components. Tumour formation requires at least two different insults: an initiator, usually a genetic transformation and one or more tumour promoters, that typically cause aberrant proliferation. The immune system can prevent tumour growth in three ways. First, it can protect the host from virus-induced tumours by eliminating or suppressing viral infections. Second, the timely elimination of pathogens and resolution of inflammation can prevent the creation of an inflammatory environment conducive to tumorigenesis. Finally, the immune system can specifically identify and destroy tumour cells on the basis of the expression of tumour-specific antigens that differentiate them from their non-transformed counterparts or molecules induced by cellular stress. This latter process is referred to as tumor immune surveillance[1,2]. Evidence supporting this model comes out from studies in mice lacking critical components of both innate and adaptive immune system. Indeed, RAG knock out (which cannot somatically rearrange lymphocyte antigen receptors and therefore cannot produce peripheral α/β T cells, B cells, NKT cells) and SCID mice (which lack T and B cells) develop spontaneous adenocarcinoma and are more susceptible to

tumor induction by MCA[3,4]. Similar findings were observed in nude mice[5]. Moreover in mice that were also defective for STAT1, an important mediator of signaling induced by both type I and type II IFN, cancer frequency is further increased[6,7]. Other evidence for the role of the immune system in suppressing tumour growth was revealed by mice lacking T cell and NK cell cytotoxic effector pathways[8] and in mice lacking of several cytokines[9]: both these models are able to develop spontaneous tumours. In conclusion, according to this evidence tumor cells are potentially able to generate an immune response. The relationship between cancer and the immune system is complex and dynamic.

First, we have to consider that tumor cells themselves are highly heterogeneous, due to the accumulation of an increasing number of genetic and epigenetic modifications. This means that, in any particular moment, clones with different immunogenic characteristics can arise.

Second, the immune system can act on tumor in two different ways: on one hand it has a protective role, contributing to the elimination of the highly immunogenic clones; on the other hand it may paradoxically promote tumor growth, exerting a selective pressure which favors the survival of less immunogenic clones or clones which have developed strategies to evade immune attack. This process has been described as “cancer immunoediting” and comprises three phases: Elimination, Equilibrium and Escape[10].

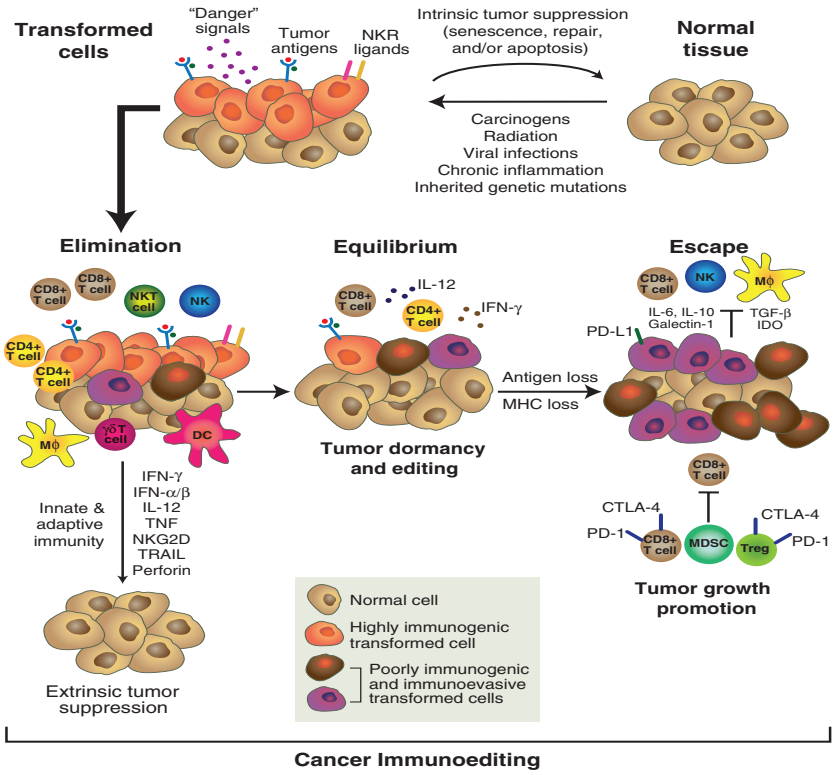

Figure 1. Cancer immunoediting is a complex mechanism that starts when the cellular transformation occurs and extrinsic tumor suppressors are involved and finish when intrinsic tumor suppressors fail. The concept of cancer immunoediting is enclosed to three phases: elimination, equilibrium and escape. In the first phase the immune cells work together to eliminate the high immunogenic transformed cells before they become clinically visible. During this phase the tumor remains in a equilibrium state which cells of the adaptive immunity are involved in the control of tumor growth. This stage can persist for years. However, the tumor cells are genetically unstable and as under pressure of immune selection they may develop variants which are no longer recognized by adaptive immunity. In this situation the tumor cells become insensitive to immune effector mechanisms or induce an immunosuppressive microenvironment. These tumor cells can enter the escape phase and their growth is not more controlled by immunity. (Figure from Robert D. Schreiber *et al. Science* 2011)

ELIMINATION: During the elimination phase, the innate and adaptive immune system work together to detect the presence of transformed cells and kill them before they becomes clinically apparent. Among the possibilities by which the immune system is alerted, it should be considered: the release of classic danger signals (such as Type I IFN), which are released by dying tumour cells or damaged tissues. This is essential for recruiting cells of the immune system such as NK, macrophages and dendritic cells. Another potential mechanism involves stress ligand such as RAE-1, which is expressed on tumour cells. These events create a microenvironment that facilitates the development of tumour specific adaptive immune responses. During this phase the infiltrating lymphocytes are stimulated to produce IFN-gamma, which have both an antiproliferative action on the developing tumor and induction of cytocidal activity in macrophages[11]. However, it also induces the production of the chemokines CXCL10 (interferon-inducible protein-10, IP-10), CXCL9 (monokine induced by IFN-γ, MIG) and CXCL11 (interferon-inducible T cell α chemoattractant, I-TAC) from the tumor cells themselves as well as from surrounding normal host tissues[12,13]. Some of these chemokines can block the formation of new vessels within the tumor leading to an increased tumor cells death[14].

Moreover, tumor cells debris produced as a result of tumor death are taken up by DCs, which migrate to lymph nodes and activate a tumor-specific immune response. Furthermore, effective elimination of cancer cells depends on specific

features of the tumour, such as its anatomic location and its rate of growth.

EQUILIBRIUM: Rare tumor cells may survive and reach the equilibrium state, in which outgrowth of tumors is specifically controlled by immune cells. During this period, many of the original escape variants of the tumor mass are destroyed, but new variants arise carrying different mutations that provide them with increased resistance to immune attack. Studies carried out in mice, in which tumor latency was induced by the re-challenge with the same tumor after the first prime[15], have shown that adaptive immunity (specifically T cells) is able to maintain the tumor in equilibrium. Additional studies with different mouse tumor cells have confirmed the role of T cells in controlling the outgrowth of tumor for a long period of time[16,17].

ESCAPE: Progression from equilibrium to the escape phase can occur through many different mechanisms, antigen loss, induction of defects in antigen processing or presentation and the induction of anti-apoptotic mechanism[18,19,20]. In this way the tumor cell variants become invisible to the immune system. The loss of tumor antigen expression is one of the best-known mechanisms of tumor immune evasion relying on the combination of genetic instability inherent in all tumor cells and on the process of immunoselection[21]. The end result is the generation of poorly immunogenic tumor cell variants that become invisible to the immune system and are able to grow

progressively. Alternatively, the escape phase is also closely associated with the establishment of an immunosuppressive state within the tumor microenvironment[22,23]. Many factors in the tumor microenvironment have been shown to contribute to tumor escape, including activation of T cells in the absence of appropriate co-stimulation, resulting in anergy[24], the expression of T cell–inhibitory molecules, such as B7-H1[25], the presence of $CD4^+CD25^+$ Tregs that suppress antitumor immunity[26], soluble suppressive factors expressed by tumors that recruit and expand immune suppressive cells such as myeloid-derived suppressor cells. Thus, tumor growth also occurs because the host immune system changes in response to increased cancer-induced immunosuppression. This process allows tumors circumventing immune recognition.

2 TUMOR MICROENVIROMENT

Tumor is a complex tissue composed of multiple cell types and components, including recruited normal cells that are involved in tumor microenvironment formation. A pivotal role in this trend is played by cells of innate immune system, especially myeloid progenitor cells, macrophages, neutrophils and cells of adaptive immune system such as T- and B-lymphocytes. In particular, three different populations have been associated to tumor formation, tumor metastasis and neoangiogenesis induction: MDSC, macrophages and neutrophils.

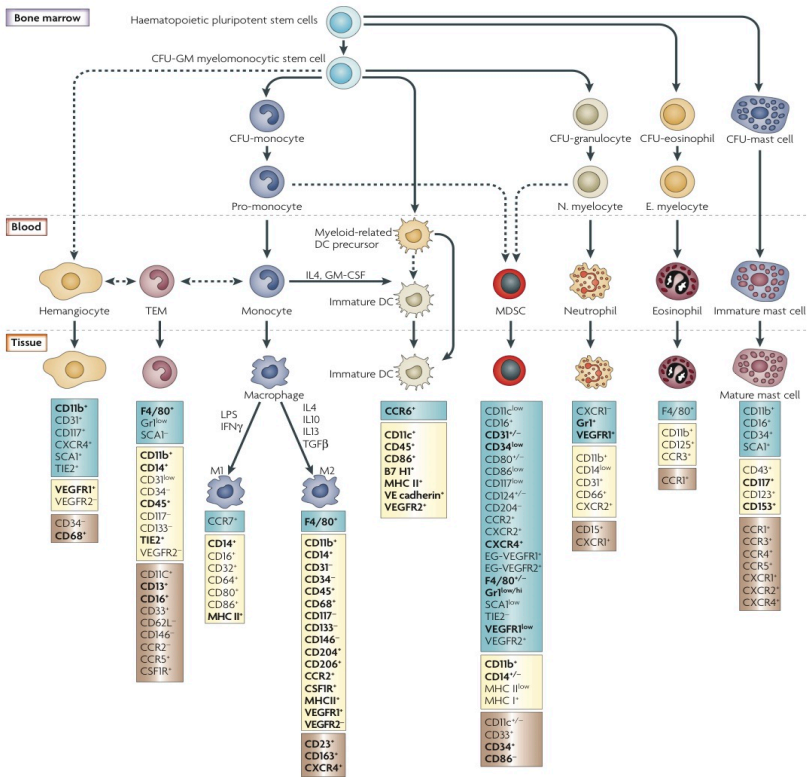

Figure 2. Expression of surface markers by various myeloid cell types. Haematopoietic stem cells differentiate into common myeloid progenitor cells and then into IMCs. Normally, IMCs in the blood exhibit a peculiar phenotype, when they enter tissues, under specific chemoattractans, they differentiate into macrophages, dendritic cells or granulocytes. However, the phenotype of each cell type may change in response to local signals, though characteristic markers are constitutively expressed. Surface markers for murine cells are shown in blue, those for human cells are in brown and those expressed by both mice and humans are in yellow. (Figure from Craig Murdoch *et al*. *Nature Reviews Cancer* 2008)

2.1 Myeloid derived suppressor cells

Myeloid-derived suppressor cells (MDSCs) are a heterogeneous population of cells of myeloid origin comprising immature macrophages, granulocytes, dendritic cells and other myeloid cells at earlier stages of differentiation, that can be identified by expression of CD11b and Gr1[27]. CD11b+Gr1+ cells comprise myeloid precursors that can generate mature granulocytes, macrophages and DCs when cultured *in vitro* under an appropriate cocktail of cytokines. In healthy mice $CD11b^{+}Gr1^{+}$ cells can be detected in sizeable numbers only in the bone marrow (about 30–40%); however, small numbers of these cells (<4%) can also be found in the blood and spleen. Instead, in cancer this population tends to accumulate preferentially in the tumor tissues and in lymphoid organs, both in mice and humans. In addition, only a third of these cells in the tumor microenvironment can differentiate into mature macrophages or DCs under appropriate *in vivo* cytokine stimuli[28,29]. In tumors, MDSCs can be characterized by the high expression of two well-known epitopes, Ly6G and Ly6C. The use of antibodies against these epitopes has allowed the identification of two MDSC subsets: a granulocytic subset expressing CD11b and Ly6G, and a monocytic subset displaying CD11b and Ly6C markers. Different studies have shown that the ability to differentiate into mature DCs and macrophages is restricted to monocytic MDSCs[30]. The expansion and activation of MDSCs is influenced by several

different factors such as COX-2[31], GM-CSF[32], M-CSF[33] and SCF[34], and cytokines, such as IL-13, IL-10 and PGEs that are released by tumors or tumor associated stromal cells. Most of these factors trigger the activation of STAT-3 that is involved in the expansion, proliferation and survival of MDSCs[35,36]. In addition, STAT-3 activation determines the up-regulation of a class of proteins, called S100, which are able to induce the inhibition of DCs and macrophage differentation[37,38]. Once recruited to tumors, MDSCs play a relevant role in tumor progression through the release of arginase-1[39], iNOS[40], ROS[41] and peroxynitrite[42] and the induction of regulatory T cells[43], that suppress the anti-tumor response of T and NK cells. Sinha and colleagues have shown that the contact between MDSCs and macrophages, results in an increase of MDSC-derived IL-10, which suppresses macrophage activity by reducing IL-12 release. However, MDSCs also appear to condition other significant events in tumor. In fact, STAT-3 has been shown to up-regulate the expression of genes involved in angiogenesis such as VEGF, bFGF, IL-1β and MMP9, which can activate endothelial cells to proliferate or induce their migration through the extracellular matrix[44]. Indeed, mice lacking STAT-3 show a delay in tumor growth. Moreover, MDSCs isolated from murine tumors express a higher level of various MMPs compared to MDSCs from healthy mice, and this stimulates tumor spreading and angiogenesis. For example, tumor cells co-injected with MDSCs expressing MMP-9 grew more rapidly and display a higher number of vessels, as compared to MDSCs from MMP-9

deficient mice. This is due to the fact that MMP9 enhances VEGF bioavailability[45]. MDSCs have also been implicated in tumor refractoriness to anti-VEGF treatment, further supporting their role in neoangiogenesis[46]. In summary, MDSCs have a complex role into tumor microenvironment, going from blocking specific T-cell activation until the formation of metastases. Therapeutic strategies to deplete in vivo MDSCs have been proposed[47], and have led to the reduction of tumor growth by the increase of anti-tumor activity of CD8 and NK cells.

2.2 MACROPHAGES

Macrophages are a heterogeneous population of cells[48] that mediate their effects not only through phagocytosis, but also through the production of various soluble factors, such as cytokines, chemokines, as well as by direct cellular contact with other cells. As blood monocytes, they migrate through the circulatory system, thus distributing to virtually all tissues of the body. Depending on their ultimate location, blood monocytes can differentiate into tissue macrophages, mature dendritic cells or osteoclasts. The markers F4/80 (mouse) and CD68 (macrosialin; human) distinguish the precursor blood monocyte from the tissue-resident macrophages. As already reported, they are present in all tissues and are involved in all aspects of immunity. Macrophages display a high degree of plasticity, in fact their phenotype is altered in the microenvironment in which

they reside. Therefore, macrophages recruited to sites of local inflammation will have a different phenotype and gene expression than macrophages recruited to the site of tumor growth. Macrophages play a critical role in the onset and progression of malignant tumors and in immune surveillance against established tumors and can determine tumor growth vs. tumor regression. Much of their ability to promote transformation and tumor progression is mediated by their ability to cause inflammation, which has long been associated with tumor development[49,50]. Macrophages can be subdivided into two subtypes: M1, which exhibit a pro-inflammatory phenotype and promote T-helper 1 responses, and M2 endowed with an immunosuppressive phenotype and promoting T-helper 2 responses[51].

Macrophages present in the tumor microenvironment, also called tumor-associated macrophages (TAM), have often an M2 phenotype. This switch occurs when the tumor begins to invade tissues, vascularize and develop[52]. Different stimuli derived from cancer cells and also from $CD4^+$ helper T cells and B cells, stimulate the tumor-promoting functions of the macrophages. Indeed, in a model of spontaneous breast carcinoma, the Th2-derived cytokines IL-4 and IL-13 induce M2 polarization of TAM[53]. Moreover, in another study, B-cells have been shown to recruit macrophages and skewing TAM by immune complexes in an M2-like direction[54]. For instance, the pleiotropic anti-inflammatory cytokines TGFβ and IL-10, IL-13 and IL-4 (derived from various sources, such as MDSCs and CD4), have been

reported to instruct the TAM[55]. TAM can be subdivided in at least two populations: M-CSFR^{+}/CD206^{neg}/MHCII^{high} that are found close to tumor blood vessels and M-CSFR^{+}/CD206^{pos}/MHCII^{low} that are found at tumor stroma borders[56]. Moreover a number of recent studies reported that many TAMs (M-CSFR^{+}/CD206^{pos}/MHCII^{low}) accumulate preferentially in the tumour-hypoxia area and they have a significant effect on neoangiogenesis by the activation of genes (mainly hypoxia-inducible factors HIF1 and HIF2) involved in this process. The induction of the transcription factors HIF-1 and -2[57,58] up-regulates VEGF[59]. Since VEGF is also a chemoattractant for macrophages, its increased synthesis leads to the accumulation of additional macrophages in hypoxic regions thereby amplifying the production of VEGF[60]. In addition, macrophages in tumor hypoxia areas show up-regulation of metalloproteinase that might have relevance in tumor metastasis. Hypoxia can also have important consequences on TAM antigen presentation activity by reducing the expression of costimulatory molecule and for this reason they are no longer able to activate cytotoxic T lymphocytes[61]. Moreover, hypoxia can up-regulate the activity of arginase 1 in TAM[62] and as in MDSC, can suppress adaptive immunity by depleting the non-essential amino acid arginine from the microenviroment. Recently, it has been shown that both chemotherapy and radiotherapy can induce the tumor to release macrophage chemoattractant factors, such as CSF-1, IL-34 and VEGF, limiting the response to the treatments[63]. The

blockade of these pathways, in combination with chemotherapy, reduces both primary tumor progression and tumour-vessel density. Therefore, TAMs are strongly correlated with poor prognosis. Based on this, therapeutic strategies aimed at eliminating, inactivating or re-polarizing them are attractive[64,65]. Studies have also shown that TAMs could be re-polarized from an M2 to an M1 phenotype. Indeed, the identification of particular genes that regulate macrophage polarization could be targets for new therapeutic approaches. One possible target is the p50 NF-kB inhibitory homodimer. p50 accumulates at very high levels in the nuclei of TAMs in wild-type mice, and over-expression of p50 blocks IL-12 production by macrophages from tumor-free mice. In contrast, macrophages from tumor-bearing mice deficient for p50 have an M1 phenotype and reduced tumor progression. Therefore, inhibition of p50 accumulation in the nucleus may re-polarize macrophages from an M2 to an M1 phenotype. Other studies have demonstrated that mice that are deficient for STAT6 produce M1 and not M2 macrophages and reject established metastatic disease and survive if their primary tumors are surgically removed[66].

Notably, a subset of monocytes expressing the angiopoietin receptor TIE2 (named TEMs) has been shown to be different from monocyte-derived macrophages[67]. TEMs circulate at low frequency in the mouse peripheral blood and have been identified in both human and mice tumors. In most cases this population was found in both perivascular and hypoxia areas. De Palma and colleagues showed that the selective depletion

of TEMs in tumor bearing mice, elicited a marked reduction of tumor angiogenesis and growth[68]. Interestingly, the elimination of TEMs did not affect the recruitment of neutrophils and TAM into the tumor, suggesting that TEMs comprise a distinct monocyte subpopulation, with strong pro-angiogenic activity[69].

2.3 NEUTROPHILS

Neutrophils play a major role in the clearance of extracellular pathogens[70]. They are essential effector cells of the innate immune response and are the most abundant immune cells. Neutrophils spend many time of their life in the bone marrow and following infections or inflammation their number increases in the circulation. The regulation of neutrophil lifespan by induction of apoptosis is critical for preventing excessive inflammation. Recently, it has been shown that neutrophils die more slowly under hypoxic conditions, a condition frequently occurring in tumors, by the up-regulation of PHD3 that regulates the expression of HIF-1[71]. Growing evidence suggest that neutrophils are influenced by the tumor microenvironment, and are involved in tumor progression, angiogenesis and metastasis. Indeed, the presence of neutrophils into the tumor is associated with poor prognosis.

It has recently been shown that the same paradigm existing for macrophage polarization can also be applied to neutrophils. Indeed, a recent study has demonstrated that pro-tumor

neutrophils can be generated by TGFβ, whereas anti-tumor ones appear following TGFβ inhibition[72], thus supporting the idea that neutrophils can be shaped *in vivo*. Another study reported on the ability of IFNβ to induce neutrophils endowed with an antitumor phenotype, while tumor-infiltrating neutrophils in IFNβ-deficient mice exhibit faster tumor growth and higher rate of vascularization[73]. These data are confirmed by the evidence showing that tumor-associated neutrophils are a major source of pro-angiogenic and metastatic factors such as Bv8, VEGF and MMP9[74,75]. Indeed, in a genetically engineered mouse model of cancer (*i.e.*, RIP1-Tag2 mice spontaneously developing pancreatic islet tumors), neutrophils have been found to express MMP9, which in turn mediates VEGF bioavailability within tumor tissues[76]. Notably, high numbers of neutrophils have been found in human tumors such as hepatocellular carcinoma where was observed a correlation between MMP9, neutrophils and angiogenesis[77].

In addition, in tumour xenograft models it has been reported that G-CSF induced up-regulation of Bv8 on neutrophils, thus promoting neoangiogenesis[78]. The pro-angiogenic activity of neutrophils has been demonstrated by specifically depleting neutrophils with antibody raised against Ly6G molecules. This deletion led to a delay in tumor growth and to a decrease of the number of vessels. Tumor-infiltrating neutrophils might also modulate adaptive anti-tumor immune responses by releasing IL-10.

3 CHEMOKINES AND CHEMOKINE RECEPTORS

Chemokines are chemotactic cytokines capable of binding seven trans-membrane proteins belonging to the family of G-protein-coupled receptors. They are small, secreted proteins mainly known to induce cell migration. They can be divided in: inducible chemokines, *i.e.,* induced during inflammation and constitutive chemokines, expressed constitutively by specific cells or tissues, the latter are important for regulating the trafficking of patrolling immune cells[79] and some of these are involved in general organogenesis[80].

Following malignant transformation, tumors can modulate their chemokine receptors and develop a distinct profile of chemokine expression[81]. Indeed, it has been shown that the induction of oncogenic signaling pathway in the tumor, may lead to the down-modulation of some chemokines and over-expression of other chemokines, which are involved in tumor growth and metastasis[82]. Several studies have shown that chemokines and growth factors are released by both tumor cells and tumor-infiltrating leukocytes, thus contributing to the complex network present within the tumor microenvironment. Indeed, tumor growth and dissemination is the result of dynamic interactions between cancer cells and components of the immune system. Thus, chemokines are not only mediators of the recruitment of different cell types to tumors; but also of the homing of tumor cells to metastatic sites. The migration to chemokine sources has been shown both *in vivo* and *in vitro* for

most of the cells present into the tumor. Indeed, the increased number of MDSCs in the tumor is due to factors, such as tumor derived CCL2, CXCL12, CXCL5 and SCF that bind to and activate their specific receptors CCR2, CXCR4, CXCR2 and CD117 on MDSCs[83,84,85]. Moreover, Bv8 released at the tumor site, might also be important for the recruitment of MDSCs through the binding to EG-VEGFR1 and EG-VEGFR2: G-protein-coupled receptors that bind both Bv8 and EG-VEGF[86]. Additionally, CXCL12 can act as a pro-angiogenic factor recruiting CXCR4-expressing endothelial precursor cells to tumor, which can be incorporated into the newly formed vessels[87].

The high number of TAMs in the tumor microenvironment is associated with the release of chemokines from tumor or stromal cells, such as CCL3, CCL4 and CCL5. These chemokines drive the recruitment of monocytes across the tumor vasculature, where they differentiate into TAMs[88,89]. Recently, the chemokine CCL2, whose expression is usually increased in tumors, has been reported to recruit inflammatory monocytes preferentially in metastatic sites, promoting their subsequent growth[90]. However, chemokines activity is not restricted only to migratory functions but also to some processes of polarization. In fact, CCL2 is able to contribute to the M2-type polarization of macrophages[91]. Interestingly, once macrophages enter the tumor, they can release by themselves chemokines that promote the invasion and metastasis of cancer cells. TAMs release chemokines close to the M2-like polarized

cells, such as CCL18 and CCL22, which are involved in metastasis and in the recruitment of T_{regs}, respectively[92,93]. Many tumors show also an increased number of infiltrating neutrophils. Their presence is often related with tumor-released CXCL8, CXCL5, CXCL2 and CXCL1, the main chemokines that bind to CXCR2 receptor expressed on neutrophils[94,95,96]. Many mediators released by neutrophils themselves are neutrophil chemottractans. Moreover, neutrophils express proteases that on one hand might activate chemokines and cytokines, whereas to the other hand, might inactivate them. One well-known protease is MMP9 that cleaves collagene to proline–glycine–proline (PGP), a peptide activating CXCR1 and CXCR2 on neutrophils. PGP might recruit neutrophils when chemokine levels are already declining[97].

Moreover, the egress of neutrophils from bone marrow into the circulation has recently been demonstrated to be mediated by the coordinated action of CXCR2 and CXCR4 receptors. Indeed, the chemokines SDF-1 and CXCL1/2, which bind CXCR4 and CXCR2 respectively, are released by endothelial cells and osteoblasts residing in the bone marrow. In the context of basal condition, the balance of these chemokines favors neutrophils retention in the bone marrow. Under acute inflammation and in tumor-bearing hosts, conditions where the production of G-CSF occurs, the balance is shifted, favoring the increase of ligands for CXCR2, ultimately promoting neutrophils release from the bone marrow[98]. In conclusion, the release of

chemokines from tumors or infiltrating immune cells is a crucial process for tumor growth.

Cell type	Major chemoattractant	Receptor
Monocyte/TAM	CCL2	CCR2
	CCL3, CLL4, CCL5	CCR1, CCR5
	VEGF, PlGF	VEGFR1, VEGFR2
TEM	CCL3, CCL5, CCL8	CCR1, CCR5
	ANGPT2	TIE2
Hemangiocytes	CXCL12	CXCR4
	VEGF	VEGFR1
MDSC	BV8	EG-VEGFR1, EG-VEGFR2
	CCL2	CCR2
	CXCL12	CXCR4
	CXCL5	CXCR2
	SCF (KIT ligand)	CD117 (KIT)
Neutrophils	CXCL8, CXCL6	CXCR1
	CXCL1, CXCL3, CXCL5, CXCL8	CXCR2
Eosinophils	CCL11	CCR3
Mast cells	SCF (KIT ligand)	CD117 (KIT)
	IL3	CD123 (IL3R)
	CCL11	CCR3
	Adrenomedullin	Unknown
Dendritic cells	CXCL12	CXCR4
	CXCL8	CXCR1, CXCR2
	β-Defensin	CCR6
	VEGF	VEGFR2

Figure 3. Released chemokines that bind chemokine receptors expressed by immune cells. (Figure from Craig Murdoch *et al*. *Nature Reviews Cancer* 2008)

4 Oxysterols and LXR nuclear receptors

Oxysterols are oxidized sterols derived from either enzymatic or non-enzymatic oxidation of cholesterol. Many different oxysterols are known, all of which sharing a cholesterol structure with oxygen-containing functional groups, such as hydroxyl, keto or epoxyde groups. Oxysterols are intermediates in cholesterol catabolism, especially in bile acids and steroid hormones synthesis. Moreover these compounds are now thought to have a role in the regulation of genes involved both in lipid and glucose metabolisms [99,100,101]. Since oxysterols have hydrophilic moieties they can easily across the cell membranes, so that in healthy humans or animals, they are poorly present in the blood. Recently, several studies have shown that oxysterols are associated with various types of tumors and can be increased in pathologic conditions.

Oxysterols have been identified as ligands for the Liver Nuclear Receptors (LXRs), especially 22R-hydroxycholesterol, 24S-hydroxycholestrol and 27-hydroxycholesterol. LXRs belong to the superfamily of structurally conserved, ligand-dependent transcription factors that are involved in diverse aspects of development, homeostasis and metabolism. This superfamily of nuclear receptors have at least five domains: a) a N-terminal regulatory domain, which contains the transcription activation function and is responsible for target gene expression; b) a DNA-binding domain containing two zinc fingers that bind to specific sequences of DNA; c) a highly variable region; d) a

ligand binding domain, highly conserved among nuclear receptors; e) a C-terminal domain with regulatory function. Two classes of nuclear receptors exist based on their localization: the first class, is present in the cytosol and upon activation form homodimers, translocate to the nucleus and activate transcription, whereas the second class, which resides in the nucleus and bind to DNA as heterodimers with an obligate partner, such as retinoid X receptor-α (RXRα), RXRβ, or RXRγ. LXRs belong at this latest class of nuclear receptor[102,103]. There are two isoforms of LXRs with homology but different expression patterns: LXRβ which is ubiquitously expressed in all cells of our body, and LXRα whose expression is restricted to the liver, adipose tissue, lung, intestine, kidney and in immune cells such as macrophages and DCs.

LXRs control cholesterol homeostasis through the activation of genes involved in cholesterol efflux, bile acids production, fatty acid synthesis and several lipid carriers[104]. After activation, LXRs bind to LXR response elements (LXRE), promoting expression or up-regulation of several genes. Some of the target genes induced by oxysterols, include ATP binding cassette transporter (ABC) such as ABCA1 and ABCG1 that are important for cholesterol efflux, sterol regulatory element binding protein 1c (SREBP-1c) and genes involved in fatty acid metabolism. In recent years, LXRs have emerged as important regulators of both innate and adaptive immunity. Interestingly, the action of oxysterols depends on the engagement of LXRα or LXRβ in specific cell types. Indeed, in macrophages it has

been shown that the activation of LXRα is essential for both apoptotic cell clearance and the maintenance of immune tolerance by transrepression of inflammatory genes. Other authors have shown that LXR activation can inhibit the expression of NF-kB target genes such as iNOS, IL-6, COX-2 and MMP9 in activated macrophages[105,106,107]. These studies were carried out in macrophages lacking either LXRα or LXRβ, suggesting that both receptors are involved in the repression of inflammatory genes. In addition, Tontonoz and colleagues reported that the engagement of LXRβ during T cells activation negatively affects their expansion, whereas loss of LXRβ confers them a proliferative advantage[108]. Our group has recently demonstrated that human and mouse tumors are able to produce LXR ligands, which bind LXRα and inhibit CCR7 expression on maturing DCs, thus dampening their migration to tumor-draining lymph nodes and activation of tumor-specific T cells. Notably, the genetic inactivation of LXR ligands *in vivo*, by overexpression of the oxysterol inactivating enzyme sulfotransferase2B1b, restored the antitumor immune response by restoring DC migration to draining lymph nodes[109].

The investigation reported in this thesis describes a new function of oxysterols in promoting tumor growth, which is however independent of the engagement of LXRs.

REFERENCES

1. Dunn, G.P., Bruce, A.T., Ikeda, H., Old, L.J., and Schreiber, R.D. 2002. Cancer immunoediting: from immunosurveillance to tumor escape. Nat. Immunol. 3:991–998.

2. Dunn, G.P., Old, L.J., and Schreiber, R.D. 2004. The three Es of cancer immunoediting. Annu. Rev. Immunol. 22:329–360.

3. Engel, A.M., Svane, I.M., Rygaard, J., and Werdelin,O. 1997. MCA sarcomas induced in scid mice are more immunogenic than MCA sarcomas induced in congenic, immunocompetent mice. Scand. J. Immunol. 45:463–470.

4. Bosma, G.C., Custer, R.P., and Bosma, M.J. 1983. A severe combined immunodeficiency mutation in the mouse. Nature. 301:527–530.

5. Svane, I.M., et al. 1996. Chemically induced sarco- mas from nude mice are more immunogenic than similar sarcomas from congenic normal mice. Eur. J. Immunol. 26:1844–1850.

6. Shankaran, V., et al. 2001. IFNgamma and lymphocytes prevent primary tumour development and shape tumour immunogenicity. Proc. Natl. Acad. Sci. U. S. A. 10:1107–1111.

7. Street, S.E., Trapani, J.A., MacGregor, D., and Smyth, M.J. 2002. Suppression of lymphoma and epithelial malignancies effected by interferon gamma. J. Exp. Med. 196:129–134.

8. van den Broek, M.E., et al. 1996. Decreased tumor surveillance in perforin-deficient mice. J. Exp. Med. 184:1781–1790.

9. Liu, J., Xiang, Z., and Ma, X. 2004. Role of IFN regulatory factor-1 and IL-12 in immunological resis- tance to pathogenesis of N-methyl-N-nitrosourea- induced T lymphoma. J. Immunol. 173:1184–119

10. G. P. Dunn, L. J. Old, R. D. Schreiber, Immunity 21, 137 (2004).

11. Bromberg, J.F., Horvath, C.M., Wen, Z., Schreiber, R.D. & Darnell, J.E. Jr. Transcriptionally active Stat1 is required for the antiproliferative effects of both interferon α and interferon γ. *Proc. Natl. Acad. Sci. USA* **93**, 7673−7678

12. Luster, A.D. & Ravetch, J.V. Biochemical characterization of a γ interferon-inducible cytokine (IP-10). *J. Exp. Med.* **166**, 1084−1097 (1987)

13. Cole, K.E. *et al*. Interferon-inducible T cell α chemoattractant (I-TAC): a novel non-ELR CXC chemokine with potent activity on activated T cells through selective high affinity binding to CXCR3. *J. Exp. Med.* **187**, 2009−2021 (1998)

14. Luster, A.D. & Leder, P. IP-10, a -C-X-C- chemokine, elicits a potent thymus-dependent antitumor response *in vivo*. *J. Exp. Med.* **178**, 1057−1065 (1993).

15. J. D. Farrar et al., J. Immunol. 162, 2842 (1999)

16. S. Loeser et al., J. Exp. Med. 204, 879 (2007).

17. J. Eyles et al., J. Clin. Invest. 120, 2030 (2010)

18. M. D. Vesely, M. H. Kershaw, R. D. Schreiber, M. J. Smyth,Annu. Rev. Immunol. 10.1146/annurev-immunol-031210-101324 (2011).

19. M. J. Smyth, G. P. Dunn, R. D. Schreiber, Adv. Immunol. 90, 1 (2006)

20. L. Zitvogel, A. Tesniere, G. Kroemer, Nat. Rev. Immunol. 6, 715 (2006).

21. Campoli, M., Chang, C.C., and Ferrone, S. 2002. HLA class I antigen loss, tumor immune escape and immune selection [review]. Vaccine. 20(Suppl. 4):A40–A45.

22. S. Radoja, T. D. Rao, D. Hillman, A. B. Frey, J. Immunol. 164, 2619 (2000)

23. R. M. MacKie, R. Reid, B. Junor, N. Engl. J. Med. 348, 567 (2003).

24. Schwartz, R.H. 2003. T cell anergy. Annu. Rev. Immunol. 21:305–334.

25. Dong, H., et al. 2002. Tumor-associated B7-H1 promotes T-cell apoptosis: a potential mechanism of immune evasion. Nat. Med. 8:793–800.

26. Terabe, M., and Berzofsky, J.A. 2004. Immunoregulatory T cells in tumor immunity. Curr. Opin. Immunol. 16:157–162.

27. Gabrilovich, D.I. and Nagaraj, S. (2009) Myeloid-derived suppressor cells as regulators of the immune system. Nat. Rev. Immunol. 9, 162– 174

28. Kusmartsev, S. & Gabrilovich, D. I. Inhibition of myeloid cell differentiation in cancer: The role of reactive oxygen species. J. Leukoc. Biol. 74, 186–196 (2003)

29. Li,Q.,Pan,P.Y.,Gu,P.,Xu,D.&Chen,S.H.Role of immature myeloid Gr-1+ cells in the development of antitumor immunity. Cancer Res. 64, 1130–1139 (2004)

30. Youn, J. I., Nagaraj, S., Collazo, M. & Gabrilovich, D. I. Subsets of myeloid-derived suppressor cells in tumor-bearing mice. J. Immunol. 181, 5791–5802 (2008).

31. Sinha, P., Clements, V. K., Fulton, A. M. & Ostrand-Rosenberg, S. Prostaglandin E2 promotes tumor progression by inducing myeloid-derived suppressor cells. Cancer Res. 67, 4507–4513 (2007).

32. Serafini, P. et al. High-dose GM-CSF-producing vaccines impair the immune response through the recruitment of myeloid suppressor cells. Cancer Res. 64, 6337–6343 (2004).

33. Bunt, S. K. et al. Reduced inflammation in the tumor microenvironment delays the accumulation of myeloid-derived suppressor cells and limits tumor progression. Cancer Res. 67, 10019–10026 (2007).

34. Pan, P. Y. et al. Reversion of immune tolerance in advanced malignancy: modulation of myeloid-derived suppressor cell development by blockade of stem-cell factor function. Blood 111, 219–228 (2008)

35. Nefedova, Y. et al. Regulation of dendritic cell differentiation and antitumor immune response in cancer by pharmacologic-selective inhibition of the janus-activated kinase 2/signal transducers and activators of transcription 3 pathway. Cancer Res. 65, 9525–9535 (2005).

36. Nefedova, Y. et al. Hyperactivation of STAT3 is involved in abnormal differentiation of dendritic cells in cancer. J. Immunol. 172, 464–474 (2004).

37. Cheng, P. et al. Inhibition of dendritic cell differentiation and accumulation of myeloid-derived suppressor cells in cancer is regulated by S100A9 protein. J. Exp. Med. 205, 2235–2249 (2008).

38. Sinha, P. et al. Proinflammatory s100 proteins regulate the accumulation of myeloid-derived suppressor cells. J. Immunol. 181, 4666–4675 (2008).

39. Bronte, V. & Zanovello, P. Regulation of immune responses by l-arginine metabolism. Nature Rev. Immunol. 5, 641–654 (2005).

40. Rivoltini, L. et al. Immunity to cancer: attack and escape in T lymphocyte–tumor cell interaction. Immunol. Rev. 188, 97–113 (2002).

41. Waris, G. & Ahsan, H. Reactive oxygen species: role in the development of cancer and various chronic conditions. J. Carcinog. 5, 14 (2006).

42. Nagaraj, S. et al. Altered recognition of antigen is a novel mechanism of CD8+ T cell tolerance in cancer. Nature Med. 13, 828–835 (2007).

43. Huang, B. et al. Gr-1+CD115+ immature myeloid suppressor cells mediate the development of tumor-induced T regulatory cells and T-cell anergy in tumor-bearing host. Cancer Res. 66, 1123–1131 (2006).

44. M. De Palma, L. Naldini, Role of haematopoietic cells and endothelial progenitors in tumour angiogenesis, Biochim. Biophys. Acta 1766 (2006) 159–166.

45. L. Yang, L.M. DeBusk, K. Fukuda, B. Fingleton, B. Green-Jarvis, Y. Shyr, L.M. Matrisian, D.P. Carbone, P.C. Lin, Expansion of myeloid immune suppressor Gr+CD11b+ cells in tumor-bearing host directly promotes tumor angiogenesis, Cancer Cell 6 (2004) 409–421.

46. F. Shojaei, X. Wu, A.K. Malik, C. Zhong, M.E. Baldwin, S. Schanz, G. Fuh, H.P. Gerber, N. Ferrara, Tumor refracto- riness to anti-VEGF treatment is mediated by CD11b+Gr1+ myeloid cells, Nat. Biotechnol. 25 (2007) 911–920

47. Suzuki, E., Kapoor, V., Jassar, A. S., Kaiser, L. R., and Albelda, S. M. (2005). Gemcitabine selec- tively eliminates splenic Gr-1+/CD11b+ myeloid suppressor cells in tumor-bearing animals and enhances antitumor immune activity. *Clin Cancer Res* 11(18):6713–6721.

48. Gordon, S., and Taylor, P. R. (2005). Monocyte and macrophage heterogeneity. *Nat Rev Immunol*5:953–964.

49. Balkwill, F., and Mantovani, A. (2001). Inflammation and cancer: back to Virchow? *Lancet* 357:539–545.

50. Balkwill, F., Charles, K. A., and Mantovani, A. (2005). Smoldering and polarized inflammation in the initiation and promotion of malignant disease. *Cancer Cell* 7:211–217

51. Allavena P, Sica A, Garlanda C et al (2008). The Yin-Yang of tumor-associated macrophages in neoplastic progression and immune surveillance. Immunol Rev 222:155–161.

52. Biswas, S. K., Sica, A. & Lewis, C. E. Plasticity of macrophage function during tumor progression: regulation by distinct molecular mechanisms. J. Immunol. 180, 2011–2017 (2008).

53. DeNardo, D.G., Barreto, J.B., Andreu, P., Vasquez, L., Tawfik, D., Kolhatkar, N., and Coussens, L.M. CD4 T cells regulate pulmonary metastasis of mammary carcinomas by enhancing protumor properties of macrophages (2009). Cancer Cell 16, 91–102.

54. Anderu, P et all. Fc activation regulates inflammation-associated squamous carcinogenesis. Cancer Cell17, 121-134 (2010)

55. Kuroda, E. et al. SHIP represses the generation of IL-3-induced M2 macrophages by inhibiting IL-4 production from basophils. J. Immunol. 183, 3652–3660 (2009).

56. Movahedi, K., Laoui, D., Gysemans, C., Baeten, M., Stangé, G., Van den Bossche, J., Mack, M., Pipeleers, D., In't Veld, P., De Baetselier, P., Van Ginderachter, J.A., 2010. Different tumor microenvironments contain functionally distinct subsets of macrophages derived from Ly6C(high) monocytes. Cancer Res. 70, 5728–5739.

57. Burke, B., Tang, N., Corke, K. P., Tazzyman, D., Ameri, K., Wells, M., and Lewis, C. E. (2002). Expression of HIF-1alpha by human macrophages: implications for the use of macrophages in hypoxia-regulated cancer gene therapy. *J Pathol* 196:204–212.

58. Talks, K. L., Turley, H., Gatter, K. C., Maxwell, P. H., Pugh, C. W., Ratcliffe, P. J., and Harris, A. L. (2000). The expression and distribution of the hypoxia-inducible factors HIF-1alpha and HIF- 2alpha in normal human tissues, cancers, and tumor-associated macrophages. *Am J Pathol* 157:411–421.

59. Jung, Y. J., Isaacs, J. S., Lee, S., Trepel, J., and Neckers, L. (2003). IL-1beta-mediated up-regulation of HIF-1alpha via an NFkappaB/COX-2 pathway identifies HIF-1 as a critical link between inflammation and oncogenesis. *FASEB J* 17:2115–2117.

60. Leek, R. D., Hunt, N. C., Landers, R. J., Lewis, C. E., Royds, J. A., and Harris, A. L. (2000). Macrophage infiltration is associated with VEGF and EGFR expression in breast cancer. *J Pathol* 190:430–436.

61. Lahat, N., Rahat, M. A., Ballan, M., Weiss-Cerem, L., Engelmayer, M., and Bitterman, H. (2003).Hypoxia reduces CD80 expression on monocytes but enhances their LPS-stimulated TNF-alphasecretion. *J Leukoc Biol* 74:197–205.

62. Doedens AL, Stockmann C, Rubinstein MP, Liao D, Zhang N, DeNardo DG, Coussens LM, Karin M, Goldrath AW, Johnson RS. Macrophage expression of hypoxia-inducible factor-1 alpha suppresses T-cell function and promotes tumor progression. *Cancer Res*. 2010 Oct 1;70(19):7465-75. Epub 2010 Sep 14

63. David G. DeNardo, Donal J. Brennan, Elton Rexhepaj, Brian Ruffell, Stephen L. Shiao, Stephen F. Madden, William M. Gallagher, Nikhil Wadhwani, Scott D. Keil,

Sharfaa A. Junaid, Hope S. Rugo, E. Shelley Hwang, Karin Jirström, Brian L. West and Lisa M. Coussens Leukocyte Complexity Predicts Breast Cancer Survival and Functionally Regulates Response to Chemotherapy *Cancer Discovery* June 2011 *1;* 54

64. Sica, A., and Bronte, V. (2007). Altered macrophage differentiation and immune dysfunction in tumor development. *J Clin Invest* 117:1155–1166.

65. Saccani, A., Schioppa, T., Porta, C., Biswas, S. K., Nebuloni, M., Vago, L., Bottazzi, B., Colombo, M. P., Mantovani, A., and Sica, A. (2006). p50 nuclear factor-kappaB overexpression in tumor- associated macrophages inhibits M1 inflammatory responses and antitumor resistance. *Cancer Res* 66:11432–11440.

66. Sinha, P., Clements, V. K., and Ostrand-Rosenberg, S. (2005b). Reduction of myeloid-derived suppressor cells and induction of M1 macrophages facilitate the rejection of established metastatic disease. *J Immunol* 174:636–645.

67. De Palma, M. et al. Tie-2 identifies a hematopoietic lineage of proangiogenic monocytes required for tumor vessel formation and a mesenchymal population of pericyte progenitors. Cancer Cell 8, 211–226 (2005).

68. De Palma, M., Venneri, M.A., Roca, C., Naldini, L., 2003. Targeting exogenous genes to tumor angiogenesis by transplantation of genetically modified hematopoietic stem cells. Nat Med 9 (6), 789–795.

69. De Palma, M., Mazzieri, R., Politi, L.S., Pucci, F., Zonari, E., Sitia, G., Mazzoleni, S., Moi, D., Venneri, M.A., Indraccolo, S., Falini, A., Guidotti, L.G., Galli, R., Naldini, L., 2008. Tumor-targeted interferon-alpha delivery by Tie2-expressing monocytes inhibits tumor growth and metastasis. Cancer Cell 14 (4), 299–311.

70. Segal, A.W. (2005) How neutrophils kill microbes. Annu. Rev. Immunol. 23, 197–223

71. Sarah R. Walmsley,Edwin R. Chilvers,Alfred A. Thompson, Kathryn Vaughan,Helen M. Marriott,Lisa C. Parker,Gary Shaw,Selina Parmar,Martin Schneider,Ian Sabroe,David H. Dockrell, Marta Milo, Cormac T. Taylor,Randall S. Johnson,Christopher W. Pugh,Peter J. Ratcliffe,Patrick H. Maxwell,Peter Carmeliet and Moira K.B. Whyte Prolyl hydroxylase 3 (PHD3) is essential for hypoxic regulation of neutrophilic inflammation in humans an mice. J. of clinical investigation (2010)

72. Fridlender, Z.G. et al. Polarization of tumor-associated neutrophil phenotype by TGF-b: “N1” versus “N2” TAN. Cancer Cell 16, 183–194 (2009).

73. Jablonska, J., Leschner, S., Westphal, K., Lienenklaus, S. & Weiss, S. Neutrophils responsive to endogenous IFN-b regulate tumor angiogenesis and growth in a mouse tumor model. J. Clin. Invest. 120, 1151–1164 (2010).

74. Coussens, L. M., Tinkle, C. L., Hanahan, D. & Werb, Z. MMP-9 supplied by bone marrow-derived cells contributes to skin carcinogenesis. Cell 103, 481–490 (2000).

75. Bergers, G. et al. Matrix metalloproteinase-9 triggers the angiogenic switch during carcinogenesis. Nature Cell Biol. 2, 737–744 (2000).

76. Nozawa, H., Chiu, C. & Hanahan, D. Infiltrating neutrophils mediate the initial angiogenic switch in a mouse model of multistage carcinogenesis. Proc. Natl Acad. Sci. USA 103, 12493–12498 (2006).

77. Kuang, D.M. et al. Peritumoral neutrophils link inflammatory response to disease progression by

fostering angiogenesis in hepatocellular carcinoma. J. Hepatol. 54, 948–955 (2011).

78. Shojaei, F., Singh, M., Thompson, J.D. & Ferrara, N. Role of Bv8 in neutrophil-dependent angiogenesis in a transgenic model of cancer progression. Proc. Natl Acad. Sci. USA 105, 2640–2645 (2008).

79. Johansson-Lindbom, B. & Agace, W.W. Generation of gut-homing T cells and their localization to the small intestinal mucosa. Immunol. Rev. 215, 226–242 (2007).

80. Muller, G., Reiterer, P., Hopken, U.E., Golfier, S. & Lipp, M. Role of homeostatic chemokine and sphingosine-1-phosphate receptors in the organization of lymphoid tissue. Ann. NY Acad. Sci. 987, 107–116 (2003).

81. Yang, G. et al. The chemokine growth-regulated oncogene 1 (Gro-1) links RAS signaling to the senescence of stromal fibroblasts and ovarian tumorigenesis. Proc. Natl Acad. Sci. USA 103, 16472–16477 (2006)

82. Wislez, M. et al. High expression of ligands for chemokine receptor CXCR2 in alveolar epithelial neoplasia induced by oncogenic Kras. Cancer Res. 66, 4198–4207 (2006)

83. Sawanobori, Y. et al. Chemokine-mediated rapid turnover of myeloid-derived suppressor cells in tumor-bearing mice. Blood 111, 5457–5466 (2008).

84. Yang, L. et al. Abrogation of TGF signaling in mammary carcinomas recruits Gr-1+CD11b+ myeloid cells that promote metastasis. Cancer Cell 13, 23–35 (2008).

85. Pan, P. Y. et al. Reversion of immune tolerance in advanced malignancy: modulation of myeloid-derived suppressor cell development by blockade of stem-cell factor function. Blood 111, 219–228 (2008).

86. LeCouter, J., Zlot, C., Tejada, M., Peale, F. & Ferrara, N. Bv8 and endocrine gland-derived vascular endothelial growth factor stimulate hematopoiesis and hematopoietic cell mobilization. Proc. Natl Acad. Sci. USA 101, 16813–16818 (2004).

87. Kryczek, I. et al. CXCL12 and vascular endothelial growth factor synergistically induce neoangiogenesis in human ovarian cancers. Cancer Res. 65, 465–472 (2005).

88. Scotton, C., Milliken, D., Wilson, J., Raju, S. & Balkwill, F. Analysis of CC chemokine and chemokine receptor

expression in solid ovarian tumours. Br. J. Cancer 85, 891–897 (2001).

89. Loberg, R. D. et al. CCL2 as an important mediator of prostate cancer growth in vivo through the regulation of macrophage infiltration. Neoplasia 9, 556–562 (2007).

90. Bin-Zhi Qian, Jiufeng LI, Hui Zang, Takanori Kitamura, Jinghang Zhang, Liam R. Campion, Elizabeth A. Kaiser, Linda A.Snyder and Jeffery W. Pollard CCL2 recruits inflammatory monocytes to facilitate breast-tumour metastasis. Nature (2011)

91. Biswas, S.K., and Mantovani, A. (2010). Nat. Immunol. 11, 889–896.

92. Chen, J., Yao, Y., Gong, C., Yu, F., Su, S., Chen, J., Liu, B., Deng, H., Wang, F., Lin, L., et al. (2011). Cancer Cell 19, this issue, 541–555.

93. Curiel,TJ. et all Specific recruitment of regulatory T cells in ovarian carcinoma fosters immune privilege and predicts reduced survival. Nat. Med. 10, 942-949 (2004)

94. Luan, J. et al. Mechanism and biological significance of constitutive expression of MGSA/GRO chemokines in

malignant melanoma tumor progression. J. Leukoc. Biol. 62, 588–597 (1997).

95. Lee, L. F. et al. IL-8 reduced tumorigenicity of human ovarian cancer in vivo due to neutrophil infiltration. J. Immunol. 164, 2769–2775 (2000).

96. Keeley, E._C., Mehrad, B. & Strieter, R._M. CXC chemokines in cancer angiogenesis and metastases. Adv. Cancer Res. 106, 91–111 (2010).

97. Gaggar, A. et al. (2008) A novel proteolytic cascade generates an extracellular matrix-derived chemoattractant in chronic neutrophilic inflammation. J. Immunol. 180, 5662–5669

98. Eash, K.J. et al. (2010) CXCR2 and CXCR4 antagonistically regulate neutrophil trafficking from murine bone marrow. J. Clin. Invest. 120, 2423–2431

99. Schroepfer Jr., G.J., 2000. Oxysterols: modulators of cholesterol metabolism and other processes. Physiol. Rev. 80, 361–554.

100. Nico Mitro, Puiying A. Mak, Leo Vargas, Cristina Godi, Eric Hampton, Valentina Molteni, Andreas Kreusch

& Enrique Saez The nuclear receptor LXR is a glucose sensor *Nature* 11 January 2007

101. Lehmann J.M., S.A. Kliewer, L.B. Moore, T.A. Smith-Oliver ,B.B. Oliver, J.L. Su, S.S. Sundseth, D.A. Winegar, D.E. Blanchard, T.A. Spencer, and T.M. Wilson. 1977. Activation of the nuclear receptor LXR by oxysterol defines a new hormone response pathway. *J Biol Chem*. 272:3137-3134

102. Janowski, B.A.,PM.j. Grogan, S.A. Jones, G.B. Wisely, S.A. Kliewer, E.J. Corey, and D.J. Mangelsdorf. 1999. Structural requirements of ligands for the oxysterol liver X receptors LXRalpha and LXRbeta. *Proc Natl Acad Sci* USA.96:266-271

103. Repa, J.J., Mangelsdorf, D.J., 2000. The role of orphan nuclear receptors in the regu- lation of cholesterol homeostasis. *Annu. Rev. Cell Dev. Biol.* 16, 459–481.

104. S. Ducheix, J.M.A. Lobaccaro, P.G. Martina, H. Guillou, Liver X Receptor: an oxysterol sensor and a major player in the control of lipogenesis *Chemistry and Physics of Lipids* 164 (2011) 500–514

105. Christopher K. Glass and Sumito Ogawa Combinatorial roles of nuclear receptors in inflammation and immunity *NATURE REVIEWS* | Immunology JANUARY 2006

106. Noelia A-Gonzalez, S.J. Bensinger, C.Hong, S. Beceiro, M.N. Bradley, N. Zelcer, J. Deniz, C. Ramirez, M. Dıaz, G. Gallardo, C. Ruiz de Galarreta,J. Salazar, F. Lopez, P. Edwards, J. Parks, M. Andujar, P. Tontonoz, and A. Castrillo Apoptotic Cells Promote Their Own Clearance and Immune Tolerance through Activation of the Nuclear Receptor LXR *Immunity* 31, 245–258, August 21, 2009

107. Castrillo, A., Joseph, S. B., Marathe, C., Mangelsdorf, D. J. & Tontonoz, P. Liver X receptor-dependent repression of matrix metalloproteinase-9 expression in macrophages. *J.Biol. Chem*. 278, 10443–10449 (2003).

108. Besinger,S.J., M.N. Bradley, S.B Joseph, N.Zelcer, E.M Janssen, M.A. Hausner, R.Shih, J.S. Parks, P.A, Edwards, B.D. Jamieson, and Tontonoz.2008. LXR signaling couples stereol metabolism to proliferation in the acquired immune response. *Cell*. 134:97-111

109. Villablanca, E. J. et al., Tumor-mediated liver X receptor-alpha activation inhibits CC chemokine receptor-7 expression on dendritic cells and dampens antitumor responses. Nature medicine 16 (1), 98.

Scope of the thesis

Aim of this project is to investigate the relationship between tumor-released LXR ligands and accumulation of neutrophils within tumors. Here, we report that LXR ligands behave as non-canonical chemotactic factors for neutrophils through the engagement of CXCR2 chemokine receptor. Moreover, we find that accumulation of neutrophils within the tumor is responsible for tumor growth by promoting neoangiogenesis. This finding might lead in near future to the identification of new treatments for cancer therapy.

Chapter 2

Tumour-released Liver X Receptor ligands attract tumour promoting neutrophils in a CXCR2 dependent manner

Laura Raccosta[1], Raffaella Fontana[1*], Daniela Maggioni[1*], Claudia Lanterna[1], Eduardo J. Villablanca[2], Andrea Leiva[1], Elena Chiricozzi[3], Maria Letizia Trincavelli[4], Simona Daniele[4,5], Claudia Martini[4], Jan-Ake Gustafsson[6,7], Knut R. Steffensen[6], Claudio Doglioni[8,9], Safiyè Gonzalvo Feo[10], Laura Mauri[3], Cristina Sensi[11], Alessandro Prinetti[3], Sandro Sonnino[3], Ivano Eberini[11], J. Rodrigo Mora[2], Claudio Bordignon[9,12], Silvano Sozzani[10,13], Catia Traversari[12,14] & Vincenzo Russo[1,14]

[1]Cancer Gene Therapy Unit, Program of Immunology and Bio Immuno Gene Therapy of Cancer, Division of Molecular Oncology, Scientific Institute San Raffaele, Milan, Italy. [2]Gastrointestinal Unit, Massachusetts General Hospital, Boston, Massachusetts. [3]Department of Medical Chemistry, Biochemistry and Biotechnology, Center of Excellence on Neurodegenerative Diseases, University of Milan, Segrate, Italy. [4]Department of Psychiatry, Neurobiology, Pharmacology and Biotechnology. University of Pisa. Pisa, Italy. [5]Department of Drug Discovery and Development, Istituto Italiano di Tecnologia, Genoa. Italy. [6]Department of Biosciences and Nutrition, Karolinska Institute, Novum, Huddinge, Sweden. [7]Center for Nuclear Receptors and Cell Signalling, University of Houston, Houston, Texas, USA. [8]Department of Pathology, Scientific Institute San Raffaele, Milan. Italy. [9]Università Vita-Salute San Raffaele, Milan, Italy. [10]Istituto Clinico Humanitas IRCCS, Rozzano, Italy. [11]Proteomics and Protein Structure Study Group, Department of Pharmacological Sciences, University of Milan, Italy. [12]MolMed S.p.A., Milan, Italy. [13]Department of Biomedical Sciences and Biotechnology, University of Brescia, Brescia, Italy. [14]These authors contributed equally to this work. [*]These authors contributed equally to this work.

SUBMITTED

ABSTRACT

Tumour formation is the result of molecular alterations involving cellular regulators[1] as well as the ability of tumor cells to affect the tumor microenvironment through smoldering inflammation[2,3], or even taking advantage of inflammation to grow and metastasize[4,5]. Tumour microenvironment is composed of various cell types, among them neutrophils are recognized as playing an important pro-tumorigenic role[6,7,8], by promoting neoangiogenesis[9,10] and/or by suppressing antitumor immune responses[11]. We have recently shown that ligands of liver X receptors (LXRs)[12], which are involved in cholesterol homeostasis[12] and in modulating immune responses[13], are released by cancer cells and suppress antitumor immune responses by dampening dendritic cell migration to draining lymph nodes[14]. Here, we report that natural and tumour-derived LXR ligands attract a subpopulation of bone marrow (BM)-derived cells in a LXR independent, CXCR2 dependent manner. These cells have phenotypic ($CD11b^{high}Gr1^{high}Ly6G^{+}$) and morphological features of neutrophils and favour initial tumour angiogenesis. Moreover, the *in vivo* inactivation of LXR ligands, the depletion of neutrophils, as well as the pharmacologic and genetic inactivation of CXCR2 inhibit neutrophil recruitment to the tumour and delay tumour growth. Our data reveal an unanticipated chemoattractant role for tumour-derived LXR ligands in promoting tumour growth that relies on the CXCR2-mediated recruitment of neutrophils, thus identifying a new therapeutic target for cancer patients.

RESULTS

We have recently shown that tumor-released LXR ligands dampen antitumor immune responses by inhibiting the migration of dendritic cells to draining lymph nodes[14]. Indeed, tumors engineered to express the oxysterol inactivating enzyme sulfotransferase 2B1b[15] (SULT2B1b) were delayed or rejected when infused in immunocompetent mice[14]. We asked whether LXR ligands were affecting other cell components of tumor microenvironment. FACS analysis of tumor infiltrating cells showed a higher percentage and number of $CD11b^{high}Gr1^{high}$ cells infiltrating the mock-transduced mouse RMA lymphoma (RMA-Mock) as compared to SULT2B1b-transduced tumors (RMA-SULT2B1b) (Fig. 1a-c and Supplementary Fig. 1a). Several tumors release LXR ligands, as evaluated by a luciferase-based assay measuring LXR activation (Fig. 1d). Among them, we analyzed the Lewis lung carcinoma (LLC) and found a higher percentage of $CD11b^{high}Gr1^{high}$ cells infiltrating LLC-Mock as compared to LLC-SULT2B1b (Fig. 1e and Supplementary Fig. 1b). To understand whether the accumulation of these cells was due to local proliferation or to their continuous recruitment from circulation, we carried out parabiosis experiments with $CD45.1^{+}$ and $CD45.2^{+}$ mice, surgically joined to establish common blood circulation[16] (Fig. 1e). Seven days after RMA challenge in $CD45.2^{+}$ mice, we separated the mice and analyzed tumor infiltrating cell chimerism by FACS (Fig. 1f). As early as 2 days after separation we observed a nearly complete disappearance of

donor CD45.1^{+}CD11b^{high}Gr1^{high} cells (Fig. 1f, g), thus indicating that these cells are continuously recruited to the tumor site. These results suggest that LXR ligands may behave as chemoattractants for CD11b^{high}Gr1^{high} myeloid cells.

We speculate that CD11b^{high}Gr1^{high} myeloid cells have a BM origin. Hence, we evaluated whether LXR ligands indeed attract BM cells, performing *in vitro* migration assays. Total BM cells from naïve mice migrated to the LXR ligand 22R-Hydroxycholesterol (22R-HC), but not to the inactive isomer 22S-HC (Fig. 2a). To identify the migrating subset of BM cells, we purified and tested the CD11b^{+} and CD11b^{-} populations. Migratory cells were in the CD11b^{+} cell fraction (Fig. 2b and data not shown). In particular, we observed that within this fraction the non-migrating cells co-expressed CD11b and Gr1 markers at intermediate levels (CD11b^{+}Gr1^{+} cells), whereas migrating cells were CD11b^{high}Gr1^{high} (Supplementary Fig. 2a), resembling the population detected *in vivo* (Fig. 1a).

Among the oxysterols tested 27-HC, 19-HC and 25-HC also induced cell migration even if to a lesser extent than 22R-HC (Supplementary Fig. 3a). On the contrary, cholesterol, some sterol-derived nuclear receptor ligands and the synthetic LXR ligand T0901317 (T1317) were unable to induce cell migration (Supplementary Fig. 3b). To identify the hydroxycholesterol species released by tumor cells, we performed solid-phase extraction of conditioned medium from RMA and NIH-3T3 cells ($8x10^5$ cells/ml/48 hours), the latter being unable to activate LXR (data not shown), followed by MS analysis. Cholesterol

oxidation products share a common fragmentation pattern during MS chemical ionization, as reported at http://www.lipidmaps.org. The analysis of hydroxycholesterol extracts from control medium or from NIH-3T3 and RMA conditioned medium showed the same qualitative fragmentation pattern (Supplementary Fig. 4a,b), in agreement with the presence of hydroxycholesterols in the fetal calf serum used to supplement the culture media[17]. Nevertheless, we observed a higher content of hydroxysterols in RMA conditioned medium than in culture medium and in NIH-3T3 conditioned medium (10 and 5.5 fold, respectively). In particular, the concentrations of hydroxycholesterols, reported as relative abundance of the 3 molecular ions (m/z 385, 369, 367) using as standard 1 mM hydroxycholesterol mixture (Supplementary Fig. 5a), were 0.195±0.012 µmol/ml, 0.357±0.027 µmol/ml and 1.973±0.34 µmol/ml, for culture medium, NIH-3T3 and RMA, respectively (Supplementary Fig. 5b). This corresponds to approximately 50-75 µmol of total oxysterols in the microenvironment of a 14-day tumor (*i.e.*, 20-30x10^6 cells), a concentration able to drive neutrophil migration. The main hydroxycholesterols contained in the RMA conditioned medium were determined by HPLC analysis using a series of standards (Supplementary Fig. 5c). Two main hydroxysterols could be identified on the basis of the retention time: the 22-HC and 27-HC in a ratio of 4:1 (Supplementary Fig. 5d). A mix of the two oxysterols was indeed able to induce a significant migration of $CD11b^{high}Gr1^{high}$ cells (Supplementary Fig. 5e). To demonstrate that 22R-HC

was able to recruit $CD11b^{high}Gr1^{high}$ cells *in vivo*, we injected mice with matrigel plugs containing 22R-HC or 22S-HC. Eighteen hours later, matrigel plugs containing 22R-HC showed a higher percentage and number of $CD11b^{high}Gr1^{high}$ cells than plugs containing 22S-HC (Fig. 2c, d). To prove that tumour-derived LXR ligands were involved in the migration of $CD11b^{high}Gr1^{high}$ cells *in vivo*, we injected total BM cells ($CD45.1^{+}$) in NOD-SCID mice bearing RMA-Mock or RMA-SULT2B1b. Eighteen hours later, a higher percentage and number of $CD45.1^{+}CD11b^{high}Gr1^{high}$ cells infiltrated RMA-Mock (>30%) than RMA-SULT2B1b (>10%) tumours (Fig. 2e-g). Furthermore, when we analyzed cells infiltrating LLC tumours from mice treated or not with Zaragozic Acid (ZA), an inhibitor of oxysterol production[14], we observed a strong reduction of $CD11b^{high}Gr1^{high}$ cells in the tumours from treated mice (*Lanterna et al manuscript in preparation*). These results indicate that tumour-derived LXR ligands attract BM-derived $CD11b^{high}Gr1^{high}$ cells. As the synthetic LXR ligand T1317 was not capable of triggering cell migration *in vitro* (Supplementary Fig. 3a), we asked whether LXRs were involved in this migration. $CD11b^{high}Gr1^{high}$ cells from *Lxra*$^{-/-}$, *b*$^{-/-}$ and *ab*$^{-/-}$ mice[18] migrated to 22R-HC as well as wild-type cells, indicating that LXR signalling is not required for the migration of $CD11b^{high}Gr1^{high}$ cells (Fig. 3a). The prototypic receptors involved in leukocyte migration[19] belong to the G protein-coupled receptor (GPCR) superfamily, and can be inhibited by the action of pertussis toxin (PTX). PTX inhibited the migration

of $CD11b^{high}Gr1^{high}$ cells to 22R-HC, thus demonstrating that a GPCR is responsible for the migration of these cells towards LXR ligands (Fig. 3b).

To identify the chemotactic receptor responsible for such migration, we compared at mRNA and protein levels the chemokine receptors expressed by migrating ($CD11b^{high}Gr1^{high}$) and non-migrating ($CD11b^{+}Gr1^{+}$) cells (Supplementary Fig. 2a). $CD11b^{high}Gr1^{high}$ cells expressed higher levels of *Cxcr2*, *Ccr1* and *Cxcr4* transcripts than $CD11b^{+}Gr1^{+}$ cells (Supplementary Fig. 2b). FACS analysis showed that these cells express $Ly6G^{+}$ and $Ly6b^{+}$ markers typical of immature/mature neutrophils, and confirmed the results of chemokine receptor expression (Supplementary Fig. 2c). Additionally, morphological and cytochemical analyses of the migrating cells showed the presence of nuclei similar to immature granulocytes and mature neutrophils[11] (Supplementary Fig. 2d). Yet, neutrophils purified from bone marrow migrated to synthetic and tumour-derived LXR ligands *in vitro* and *in vivo* (Supplementary Fig. 6a-c).

The recruitment of $CD11b^{high}Gr1^{high}Ly6G^{+}$ cells (hereafter referred to as BM-derived neutrophils) into tumours could be mediated by the SDF-1a/CXCR4 and CXCL5/CXCR2 axes[20], we therefore performed a migration assay towards 22R-HC, CXCL5, SDF-1a and MIP-1a, a ligand of CCR1. BM-derived neutrophils migrated to 22R-HC, CXCL5 and SDF-1a, while migration to MIP-1a was negligible (Fig. 3c). In addition, the pre-treatment of BM-derived neutrophils with 22R-HC induced the heterologous desensitisation of the cells to the subsequent

response to CXCL5, while did not affect the migration to SDF-1a (Fig. 3c). These results suggest that 22R-HC and CXCL5 may share the same chemotactic receptor, namely CXCR2. Treatments of BM-derived neutrophils with CXCL5 or with the CXCR2 antagonist SB225002[21] further demonstrated the involvement of CXCR2, as treated cells failed to migrate to CXCL5 and to 22R-HC (Supplementary Fig. 7a, b). To finally prove the role of the CXCR2 receptor, we carried out migration experiments using BM-derived neutrophils from *Cxcr2*$^{-/-}$ mice[22]. These cells did not migrate to either CXCL5 or 22R-HC, while they migrated to SDF-1a, demonstrating that CXCR2 is indeed the receptor involved in the migration of BM-derived neutrophils towards the LXR ligand 22R-HC (Fig. 3d). The engagement of CXCR2 by 22R-HC was further demonstrated by three independent experimental approaches. First, 22R-HC was able to induce CXCR2 down-regulation, as evaluated by FACS analysis (Fig. 3e). Second, 22R-HC bound and activated CXCR2, as evaluated by ^{35}S-GTPγS assay (Fig. 3f). In this experiment, 22R-HC was able to stimulate, in a concentration dependent manner, the binding of ^{35}S-GTPγS to membranes from CXCR2-expressing L1.2 cells, with an EC_{50} value of 2.42 ± 0.55 μM (Fig. 3f). On the contrary, 22S-HC did not activate any ^{35}S-GTPγS binding, suggesting that this compound does not interact with CXCR2. The natural CXCR2 ligand IL-8 induced an increased ^{35}S-GTPγS binding, with an EC_{50} of 2.50 ± 0.17 nM (Fig. 3f). We did not observe any stimulation of ^{35}S-GTPγS binding in Mock-L1.2 cells, demonstrating the specificity of the

interaction with CXCR2 (Supplementary Fig. 8a). Moreover, we observed a dose-dependent inhibition of ^{35}S-GTPγS binding when 22R-HC was displaced by increasing concentrations of the CXCR2 antagonist SB225002 (Supplementary Fig. 8b). Third, 22R-HC was able to displace ^{125}I-IL-8 from CXCR2-expressing cells in a dose-dependent manner with an IC_{50} of approximately 40 mM (Fig. 3g). 25-HC, another migration-inducing oxysterol also displaced ^{125}I-IL-8 binding (Supplementary Fig. 9); whereas 22S-HC and 4b-HC (two oxysterols unable to promote cell migration) were not active (Figure 3g and Supplementary Fig. 9). The lower displacement capabilty of 22R-HC and 25-HC as compared to IL-8 (Supplementary Fig. 9) is likely due their lower binding affinity for CXCR2, or to the interaction of the oxysterols with only one of the two binding sites on the receptor[23,24]. Indeed, structure-function studies have shown that chemokine receptor binding and activation involve two sites on CXCR2. In particular, one molecule of IL-8 is supposed to sequentially bind the N-domain residues (site-I) and the extracellular/transmembrane residues (site-II) of CXCR2[23,24]. Based on the human CXCR4 crystallographic structure[25], we built a model of CXCR2 through a classical comparative modelling approach (Supplementary Methods). According to our molecular docking simulation, carried out on the CXCR2 three-dimensional model, oxysterols are supposed to bind to CXCR2 site-II (Supplementary Figure 10 and Supplementary Table 1). The theoretical p*Ki* values measured for the 8 oxysterols tested range from 9.49 to 8.21

(Supplementary Table 2), with 22R-HC showing a 10-fold lower complex dissociation constant than 22S-HC or 4β-HC, a difference in agreement with the results of the displacement assay (Supplementary Fig. 9). Unfortunately, the crystallographic structure of CXCR4 lacks the first 25 amino acids[25], not allowing us to investigate the interaction of oxysterols with the N-terminus binding site-I.

The *in vivo* involvement of CXCR2 in neutrophil migration to tumor-derived oxysterols was demonstrated by competitive homing migration experiments, in which we observed a preferential migration of wild-type neutrophils when a mixed cell population of wild-type and *Cxcr2*$^{-/-}$ BM cells was allowed to migrate to RMA-Mock (Fig. 3g). Furthermore, we found a lower number of neutrophils infiltrating RMA tumours established in *Cxcr2*$^{-/-}$ than in wild-type chimera mice (Supplementary Fig. 11). Notably, the role of tumour-derived oxysterols in the CXCR2-dependent migration of neutrophils was supported by the observation that these cells migrated preferentially to oxysterol-releasing RMA-Mock tumours, despite they released lower levels of the CXCR2 ligands CXCL1 and CXCL5 than RMA-SULT2B1b tumours (Supplementary Fig. 12).

Neutrophils have been described as favouring tumour formation by different mechanisms, including immune suppression of antitumor responses and promotion of an initial angiogenic switch[6,9]. The addition of BM-derived neutrophils, isolated from naïve or RMA tumour-bearing mice to OVA-specific OT-I T cells[26], did not affect T cell priming (Supplementary Fig. 13a, c)

or re-stimulation *in vitro* (Supplementary Fig. 13b). However, we cannot rule out that *in situ*, within the tumour microenvironment, neutrophils might acquire immune suppressive activity[27].

Tumour angiogenesis was enhanced when BM-derived neutrophils were co-injected in matrigel admixed with RMA or B16F1 cells. Indeed, we observed by immunohistochemistry an increased number of $CD31^+$ vessels (Fig. 4a) and a higher percentage of $CD45^-CD31^+$ cells in matrigel plugs containing BM-derived neutrophils admixed with RMA (Fig. 4b) or B16F1 (Supplementary Fig. 6d). In line with these results, 22R-HC-migrating $CD11b^{high}Gr1^{high}$ cells expressed higher mRNA levels of the pro-angiogenic factor *Bv8*[28] as compared to $CD11b^+Gr1^+$ cells (Supplementary Fig. 14a), and released Bv8 when exposed for 18 hours to RMA-conditioned medium (Supplementary Fig. 14b). Thus suggesting, as shown by others[10], a role for neutrophil-released Bv8 in promoting angiogenesis.

The tumour promoting effects of the recruited neutrophils are supported by the observation that 6 days after challenge, the size of RMA tumours admixed with $CD11b^{high}Gr1^{high}$ cells was greater than that admixed with $CD11b^+Gr1^+$ cells or RMA alone (Fig. 4c), and by *in vivo* neutrophil depletion experiments. Indeed, the intratumor administration of an anti-Gr1 mAb to RMA-bearing mice induced tumour growth delay, as well as the reduction of the percentage of neutrophils and $CD45^-CD31^+$ cells (Fig. 4d-f and Supplementary Fig. 15). The role of the oxysterol-CXCR2 axis in controlling tumors is supported by the

observation that the CXCR2 antagonist SB225002 significantly delayed RMA growth in wild-type mice (Fig. 4g). However, as in the tumour microenvironment CXCR2 is expressed by neutrophils and at lower levels (data not shown) by some mature endothelial cells[29,30], we performed tumour growth experiments in wild-type and in *Cxcr2*$^{-/-}$ bone marrow chimera to distinguish the role of the two cell populations. SB220055 significantly delayed tumour growth in wild-type chimera mice, while it did not change the tumour growth rate in *Cxcr2*$^{-/-}$ chimera mice (Fig. 4h), thus suggesting that in our model tumour-released oxysterols favour tumour growth by recruiting neutrophils. Whether oxysterols may have an effect also on BM-derived endothelial progenitor cells expressing CXCR2 deserves a deeper investigation in suitable tumour models[31].

This mechanism and the previously identified LXR-dependent dampening of DC migration[14] add up to promote tumour growth; indeed in *Lxra*$^{-/-}$ bone marrow chimera, a model in which LXRa signalling is absent, the growth rate of the LXR ligand releasing RMA-Mock was higher than that of RMA-SULT2B1b (Supplementary Fig. 16). Notably, in our tumour model LXRb does not play a major role as RMA-Mock showed the same growth rate in *Lxrb*$^{-/-}$ and wild-type bone marrow chimera mice (data not shown).

Our study extends recent results on the chemoattractant role of oxysterols[32,33], and identify a new unexpected role of tumour-derived LXR ligands that recruit neutrophils in a CXCR2-dependent manner and favour tumour growth by inducing

neoangiogenesis. The demonstration that several human tumour cell lines release LXR ligands (Supplementary Fig. 17), along with the observation that higher numbers of intratumour neutrophils severely affect overall survival of kidney cancer patients[34], suggest that manipulating LXR ligands, their interaction with CXCR2 and immune cells could provide new targets for the development of therapeutic modalities to treat cancer patients.

METHODS

Animal studies and reagents. Wild-type C57BL/6 CD45.1 or CD45.2 and NOD-SCID mice were obtained from Charles River and Harland. *Cxcr*$^{+/-}$ and *Cxcr2*$^{-/-}$ mice were from Jackson Laboratory. *Lxra*$^{-/-}$ knock-out mice were generated as previously described[18]. All mice were maintained in the pathogen-free facility of San Raffaele Scientific Institute under institutionally approved protocols. All experimental work was conducted in compliance with the Institutional Animal Care and Use Committee programme. Most antibodies were from BD Pharmingen. CXCL5, SDF-1a, MIP1a and IL-8 were from R&D systems. 22R-Hydroxycholestrol(HC), 22S-HC, 25-HC, 24,25 Epoxycholesterol, 7b-HC, Cholesterol, Chenodeoxycolic Acid (CDCA) and Glyco-CDCA were from Sigma-Aldrich and from Avanti Polar Lipids. 27-HC, 4b-HC and 7a-HC were from Avanti Polar Lipids. 19-HC was from Santa Cruz. T0901317 and Pregnenolone were from Cayman. Carboxyluorescein succinimidyl ester (CFSE) and CMTMR (5-(and-6)-(((4-chloromethyl)benzoyl)amino)tetramethylrhodamine) were from Molecular Probes (Invitrogen). PTX and PTX B-Oligomer were from Alexis. Rat anti-mouse CD11b mAb-coupled magnetic MicroBeads were from Miltenyi. SB225002 was from Tocris. Dead Cell Stain Kit (Live/Dead Fixable Far Red) was from Invitrogen.

Promoter Reporter Assay for Nuclear Receptors Activity. We transiently transfected HEK293 cells ($1x10^5$ cells per well) with the reporter plasmid pMH100X4-TK-luc (100 ng per well)

together with 100 ng per well of pCMX-Gal4-LXRα or pCMX-Gal4-LXRβ plasmids using FuGene 6 Transfection Reagent (Roche). Four hours after transfection, we treated the cells with tumor-conditioned medium for 24 h. We analyzed luciferase activities by luciferase Reporter Assay Systems (Promega) according to the manufacturer's protocol. We used β-galactosidase (30 ng/well) (Invitrogen) for transfection normalization.

Chemotaxis assays. Chemotaxis assays were performed using 5-μm pore polycarbonate filters in a 24-well transwell chamber (Corning Costar Corporation). Total bone marrow or $CD11b^+$ purified cells ($2x10^5$/100 μl) were seeded in the upper chamber, whereas in the lower chamber 600 μl of medium (RPMI 0.5% BSA) containing 15 mM of 22R-HC or 22S-HC or 100 ng of CXCL5, SDF-1a, MIP1a or IL-8 was added. Two hours later, the number of cells migrated in the lower chamber was measured by flow cytometer acquisition of a fixed number of beads (10.000/sample) (Polysciences). GCPR involvement was investigated by pre-treating the cells for 90min at 37°C with PTX (500 ng). Desensitization experiments were performed by pre-treating the cells for 30-45min at RT with 22R-HC (50 mM) or CXCL5 (2 mg ml^{-1}). The cells were then washed and seeded as described before. PTX B-Oligomer (500 ng) was used as control of PTX inhibition. Experiments of inhibition with SB225002 were performed treating the cells with SB225002 (20 mM) before migration. To obtain a higher number of cells, migration was carried out using 6-well transwell chambers

(Millipore) and seeding 2 x 10^6 $CD11b^+$ purified cells in 1.6 ml of medium. Results are expressed as the percentage of migrated cells relative to cells in the input[35]. Spontaneous migration (basal values that was always below 35% of specific migration) was always subtracted with the exception of the experiments reported in Figures 2a and b.

Analysis of tumor infiltrating $CD11b^+Gr1^+$ cells. RMA-Mock, RMA-SULT2B1b, LLC-Mock and LLC-SULT2B1b have been described previously[14]. Tumors collected 14-15 days after injection were cut into small fragments and digested for 45-60min at 37°C with collagenase A, B and D (Roche) (1.4 mg ml^{-1}) and DNase (Roche) (40 mg ml^{-1}) mixture in RPMI medium with 10% FBS to get single cell suspension. Single cell suspensions were then washed and labelled with Dead Cell Stain Kit reagents for 30min at 4°C. After washing, the cells were incubated for 5min at RT with Fc-blocking solution (10 mg ml^{-1} mouse Fc Block, BD Pharmingen) and labelled with CD11b, Gr1, CD45.1 or CD45.2 mAbs. Samples were run by FACSCalibur flow cytometer (BD Biosciences) and analyzed by FlowJo software by gating on live cells.

***In vivo* migration experiments.** For experiments of bone marrow transfer, we injected NOD-SCID mice with RMA-Mock or RMA-SULT2B1b. Fifteen days later, we injected 20 x 10^6 total bone marrow cells from *wild type* mice, or bone marrow cells mixed from *wild type* and *Cxcxr2*$^{-/-}$ mice. Eighteen hours later we collected and processed tumors as described before.

We evaluated only the percentage and number of bone marrow-derived exogenous $CD11b^{high}Gr1^{high}$ cells infused.

Parabiosis experiments. Six- to eight-week old sex-matched congenic C57BL/6 wild type were joined at the flanks as described in[16]. Three days later, 5 x 10^5 RMA cells were injected s.c. in the flank of the CD45.2 mice. Mice were surgically separated 7-, 4- and 2-days prior collection of tumors and analysis.

Matrigel plug assay. Matrigel (500 ml) containing 22R-HC (0.5 mM) or 22S-HC (0.5 mM) (100 ml) was injected subcutaneously into C57BL/6 mice. Plugs were removed after 18 hours, digested for 1 hour at 37°C with Dipsase (1.8 U ml^{-1}, Gibco) and analyzed by FACS as described before.

Viral vectors and transduction procedures. The mCXCR2-ΔNGFr lentiviral transfer vector was generated by cloning the murine CXCR2 cDNA in place of the GFP cDNA into the self-inactivating hPGK.GFP.wPRE.mhCMV.ΔNGFr.SV40PA lentiviral vector (AgeI/SalI sites)[14]. Concentrated VSV-G-pseudotyped LV stocks were produced and titered[14]. L1.2 cells were transduced with $1x10^8$ or $1x10^9$ transduction units (TU)/ml VSV-G pseudotyped LV stocks, corresponding to 1.5 or 15 MOI.

Down-regulation of CXCR2. Purified $CD11b^+$ cells were treated with 50 mM of 22R-HC or 22S-HC, 2 mg ml^{-1} of CXCL5, 1 mg ml^{-1} SDF-1a, or 10 mM of SB225002 for 30min at RT. After washing the cells were labelled with anti-CD11b, anti-Gr1

and anti-CXCR2 mAbs, run by FACS and analyzed by FlowJo software.

^{35}S-GTPγS binding assay. L1.2 cells transfected with mock or with mouse CXCR2 were homogenized in 5 mM Tris–HCl and 2 mM EDTA (pH 7.4) and centrifuged at 48 000 X g for 15min at 4 °C. The resulting pellets (plasma membranes) were washed in 50 mM Tris–HCl and 10 mM MgCl2 (pH 7.4) and stored at -80°C until used. The pharmacological profile of the new ligands toward the receptor was evaluated by assessing the effect of different ligand concentrations to modulate CXCR2-G protein coupling. Briefly, aliquots of control or CXCR2 transfected cell membranes (10 μg) were incubated in 96-well plates in assay buffer (20 mM Hepes, 3 mM MgCl2,100 mM NaCl, pH 7.4) supplemented with GDP (3 μM), ^{35}S-GTPγS (0.15 nM, 1,250 Ci/mmol, Perkin Elmer) and different compound concentrations (10 nM-50 μM). The CXCR2 agonist, IL-8 (0.1-50 nM), was also assayed in parallel as reference compound. After incubation at room temperature in a shaking water bath for 60min, cells were harvested by rapid filtration and assayed for ^{35}S radioactivity. Nonspecific ^{35}S-GTPγS binding was measured with 50 μM GTPγS. For the analysis and graphic presentation of ^{35}S-GTPγS binding data, a nonlinear multipurpose curve fitting computer program (Graph-Pad Prism) was used. All data are presented as the mean ± s.e.m. of three different experiments.

Receptor binding assays. Competition for the binding of ^{125}I-labeled IL-8 ([^{125}I]IL-8; sp. act., 2200 Ci/mmol; Perkin Elmer) to mouse L1.2 cells was conducted as described previously[36].

L1.2 CXCR2- or Mock-transduced cells (0.8 x10^6/50 ml) in binding medium (RPMI 1640 with 1 mg/ml BSA) were incubated with 0.3 nM labelled chemokine in the presence of 300 nM of unlabeled IL-8, or 100 mM 22R-HC, 25-HC, 22S-HC, or 4b-HC at 4°C for 2 h. Dose-dependent inhibition experiments were performed by incubating the cells with 100, 50, 10 or 1 mM 22R-HC or 22S-HC. At the end of the incubation, cells were pelleted through a cushion of oil by microcentrifugation. The radioactivity present in the tip of the tubes was evaluated using a gamma counter. Non-specific binding to L1.2 cells Mock-transduced was always subtracted for each condition described. Data were analyzed by Prism software.

Angiogenesis assay. We injected mice with RMA tumor cells (2 x10^5) alone or admixed with either LXR ligand migrating $CD11b^{high}GR1^{high}$, or LXR ligand non-migrating $CD11b^{+}GR1^{+}$ cells (1x10^5) re-suspended in PBS (100 ml), mixed with 100 ml of matrigel. Six days after the injection, mice were sacrificed and matrigel plugs collected and digested with collagenase A, B and D (1.4 mg ml^{-1}) and Dispase (1.8 U ml^{-1}). We washed cell suspensions and and labelled with Dead Cell Stain Kit reagents for 30min at 4°C. After washing, the cells were incubated for 5min at RT with Fc-blocking solution (10 mg ml^{-1} mouse Fc Block, BD Pharmingen) and labelled with CD31, CD45 mAbs. We analyzed the samples by FACS as described before. Experiments with B16F1 were performed by injecting B16F1 cells (0.5 x10^5) alone or admixed with BM isolated neutrophils

(5 x10^5) re-suspended in PBS (100 ml), mixed with 100 ml of matrigel.

Tumor growth experiments. We injected C57BL/6 or NOD-SCID mice subcutaneously with live RMA (1 x 10^5) or LLC (3 x 10^5) tumor cells. We evaluated tumor size by measuring perpendicular diameters by a caliper. Data are reported as the average tumor volume ± s.d. We gave zaragozic acid (100 mg) (Sigma) or saline intraperitoneally contralaterally every 2 d, starting 6 d after tumor infusion. We gave SB225002 (0.8 mM) (Tocris) or DMSO intraperitoneally every 2 d, starting 5 d after tumor infusion.

Neutrophil depletion. C57BL/6 mice were injected subcutaneously with live RMA (1 x 10^5). Seven days later, we performed neutrophil depletion by intratumor injections of 30 µg of purified monoclonal anti-Ly6G antibody 1A8 (Biolegend) or Rat IgG control antibody (Jackson Immunoresearch), twice per week, as described in[11]. Tumor neutrophil depletion was confirmed at the end of the tumor challenge by flow cytometry using anti-CD11b and anti-Gr1 mAbs. Angiogenesis was evaluated by by flow cytometry using anti-CD31 and anti-CD45 mAbs. Tumor growth was analyzed as described before.

Immunohistochemistry. For immunofluorescence staining, we used anti-CD11b FITC, biotynilated anti-Gr1 antibody revealed by streptavidin, Alexa Fluor 555 (Invitrogen) and DAPI. We embedded samples in OCT freezing medium and prepared tissue sections 7 mm thick. Sections were fixed in 4%

paraformaldehyde. Slides were mounted with medium (DakoCytomation) and images were taken by Nikon Eclipsei microscope. For immunohistochemistry, we embedded tumor samples in optimal cutting temperature medium and froze them in liquid nitrogen. We stained 3-mm paraffin sections with H&E for morphological analysis or immunostained them with the rat antibody to mouse CD31 (Serotec) followed by a biotinylated-conjugated rat-specific antibody (Biocare). Reactions were visualized with horseradish peroxidase–conjugated streptavidin and 3,3 diaminobenzidine as chromogen (Biogenex).

Tumor growth in *Cxcr2*$^{-/-}$ bone marrow chimera. We transplanted lethally irradiated (11 Gy) C57BL/6 mice with bone marrow from *Cxcr2*$^{-/-}$ or wt mice (5 x10^6 bone marrow cells per mouse). Six-eight weeks later, we challenged mice with RMA with or without SB225002 (0.8 mM). *Cxcr2*$^{-/-}$ genotype was performed by PCR on splenocytes at the end of tumor challenge experiments. We noticed that mice transplanted with the bone marrow of *Cxcr2*$^{-/-}$ underwent death during the reconstitution phase. To avoid this problem, we treated transplanted mice with enrofloxacin for 15 days (7.5 mg/150 ml of Baytril 5% solution in 300 ml of drinking water).

Statistical analyses. Data are expressed as mean ± s.e.m. and were analyzed for significance by ANOVA with Dunnet's, Bonferroni's or Tukey's multiple comparison test, or by Student's *t* test. The analysis was performed with Prism software.

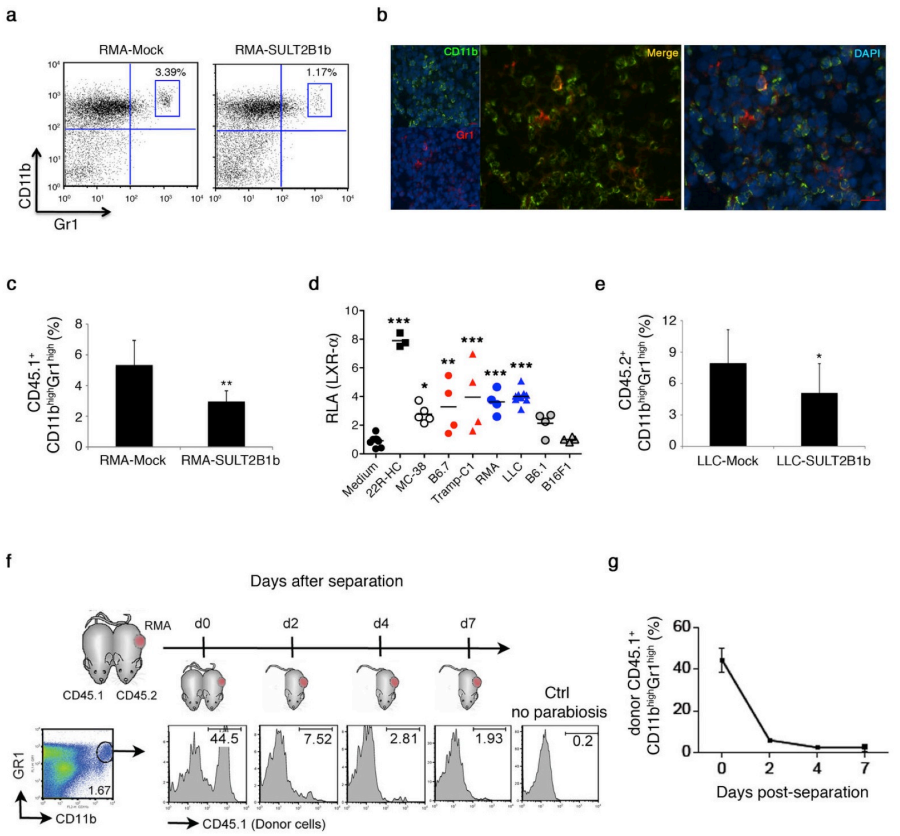

Figure 1 Tumour released LXR ligands recruit bone marrow-derived CD11b^{high}Gr1^{high} myeloid cells at the tumor site. a, Flow cytometric analysis of CD11b^{high}Gr1^{high} tumour infiltrating cells. **b**, Immunofluorescence of RMA-Mock tumour stained with anti-CD11b (green), anti-Gr1 (red) mAbs and DAPI (blue), showing CD11b+Gr1+ cells. Data represent one of four independent experiments. Scale bars, 25 μm. **c**, Percentage of CD11b^{high} Gr1^{high} cells infiltrating RMA-Mock (n = 12) and RMA-SULT2B1b (n = 11) tumors. Mean ± s.e.m. of two pooled experiments. ***P=0.0002 (Student's t-test). **d**, Luciferase assay for LXR-α activation by the indicated tumor-conditioned medium. Each symbol corresponds to a single experiment, and the line represents the mean value. *P<0.05; **P<0.01; ***P<0.0001 (Anova). RLA, relative luciferase activity. **e**, Percentage of CD11b^{high} Gr1^{high} cells infiltrating LLC-Mock and LLC-SULT2B1b tumours. Mean ± s.e.m. (n = 13 mice). *P=0.01 (Student's t-test). **f**, Parabiosis experiments. CD11b^{high}Gr1^{high} gated cells were analysed for CD45.1 marker at day 0, 2, 4 and 7 after mice separation. FACS analysis of one representative experiment is reported. **f**, Quantification of the flow cytometric analysis as in **e**, performed on three mice.

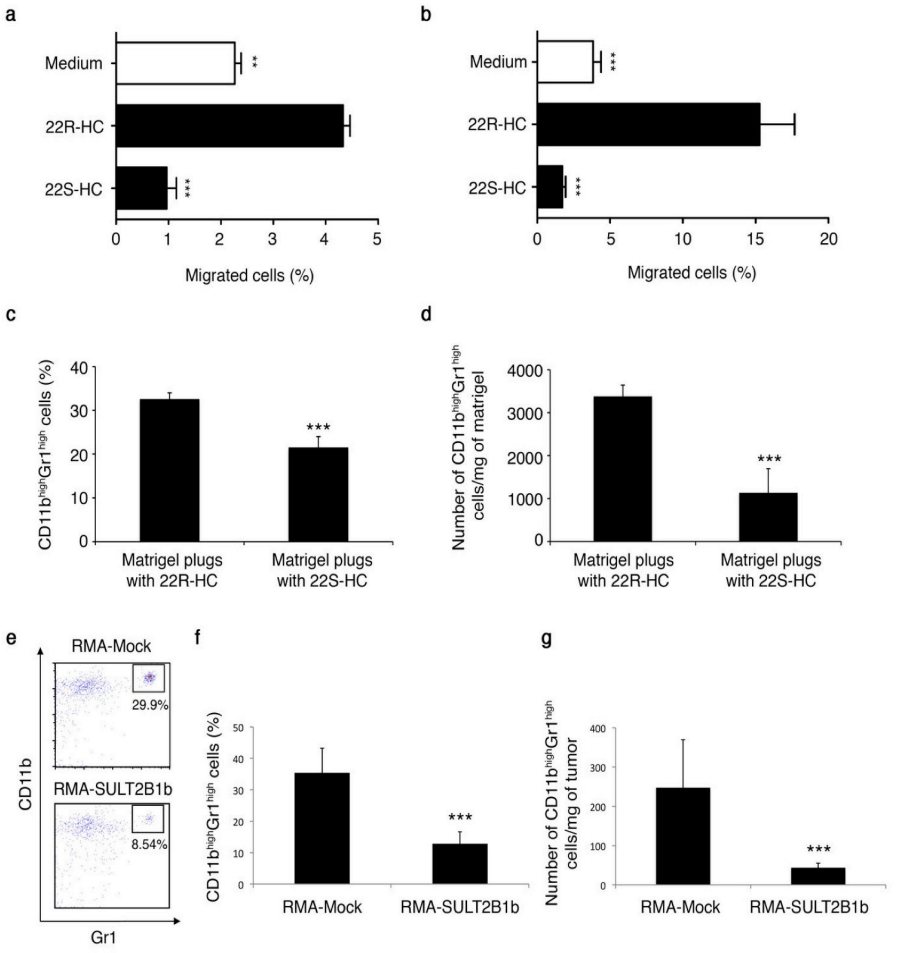

Figure 2 | **BM-derived CD11b^{high}Gr1^{high} cells migrate towards natural and tumour-released LXR ligands. a**-**b**, *In vitro* migration of total BM cells (**a**) and CD11b+ purified cells (**a**) towards 15 μM of the LXR ligand 22R-HC and the isomer 22S-HC. Mean ± s.e.m. of four pooled experiments. ***P*<0.01; ****P*<0.0001 (Anova). **c**-**d**, Percentage of CD11b^{high}Gr1^{high} cells (**c**) and number of CD11b^{high}Gr1^{high} cells/mg of matrigel (**d**) infiltrating matrigel plugs embedded with 0.5 mM of 22R-HC or 22S-HC. Data presented as mean ± s.e.m. of two pooled experiments (*n* = 5 mice). ****P*<0.0001 (Student's *t*-test). **e**, FACS analysis of CD45.1+CD11b^{high}Gr1^{high} cells infiltrating LXR-ligand producing (RMA-Mock) and non-producing (RMA-SULT2B1b) tumors, following i.v. injection of CD45.1+ BM cells. One representative experiment is shown. **f**-**g**, Percentage of CD11b^{high}Gr1^{high} cells (**f**) and number of CD11b^{high}Gr1^{high} cells/mg of tumor (**g**) infiltrating RMA- Mock or RMA-SULT2B1b are shown as mean ± s.e.m. (*n* = 7 mice). ****P*<0.0001 (Student's *t*-test).

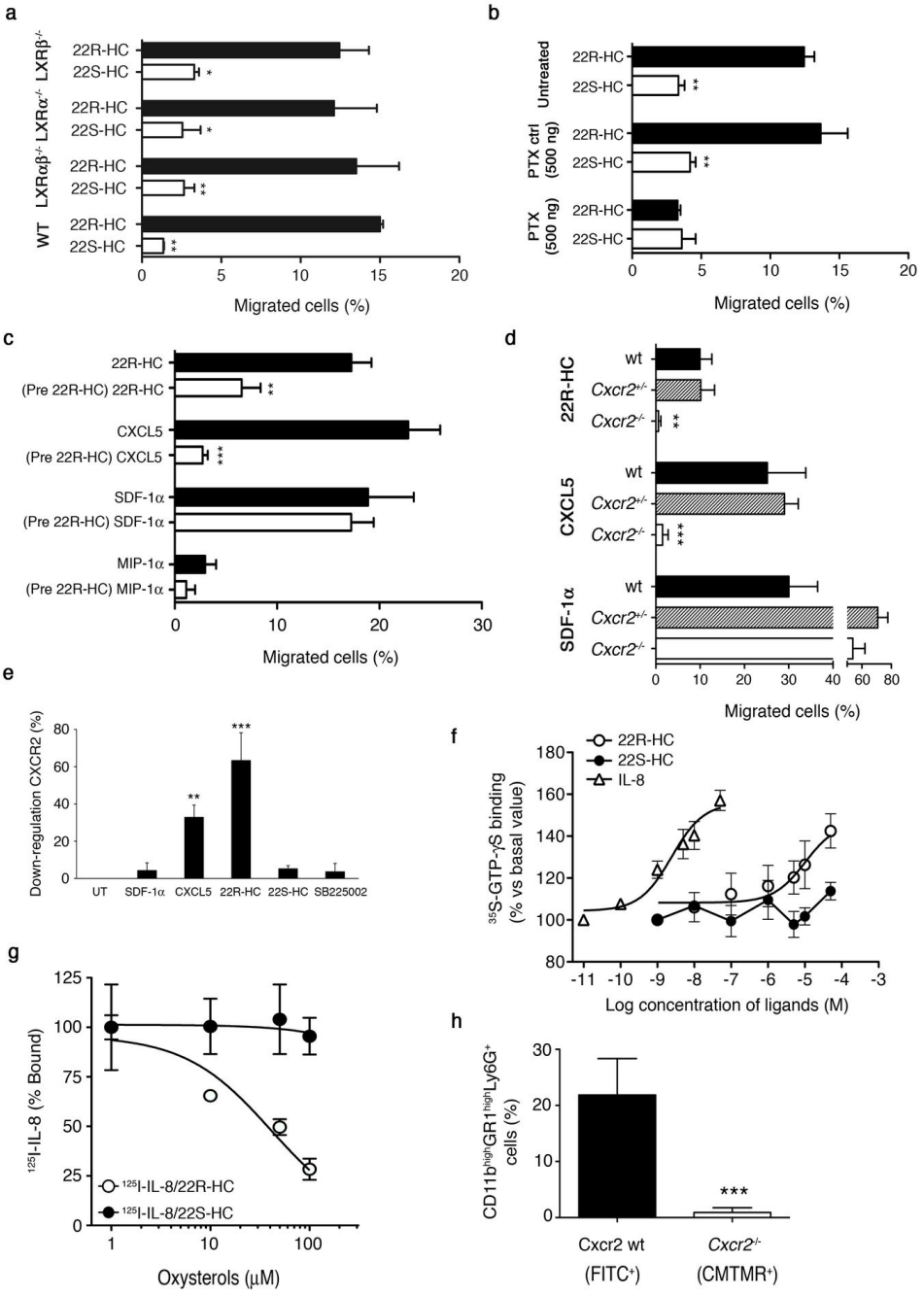
a
22R-HC
22S-HC
LXRβ-/-
LXRα-/-
LXRαβ-/-
WT
Migrated cells (%)
b
Untreated
PTX ctrl (500 ng)
PTX (500 ng)
Migrated cells (%)
c
(Pre 22R-HC) 22R-HC
CXCL5
(Pre 22R-HC) CXCL5
SDF-1α
(Pre 22R-HC) SDF-1α
MIP-1α
(Pre 22R-HC) MIP-1α
Migrated cells (%)
d
wt
Cxcr2+/-
Cxcr2-/-
22R-HC
CXCL5
SDF-1α
Migrated cells (%)
e
Down-regulation CXCR2 (%)
UT
SDF-1α
CXCL5
22R-HC
22S-HC
SB225002
f
22R-HC
22S-HC
IL-8
35S-GTP-γS binding (% vs basal value)
Log concentration of ligands (M)
g
125I-IL-8 (% Bound)
125I-IL-8/22R-HC
125I-IL-8/22S-HC
Oxysterols (μM)
h
CD11bhighGR1highLy6G+ cells (%)
Cxcr2 wt (FITC+)
Cxcr2-/- (CMTMR+)

Figure 3 | LXR ligands attract CD11b+Gr1+ cells by engaging the CXCR2 receptor. a, *In vitro* migration of CD11b+Gr1+ cells from wild-type (WT) and *Lxrs* knock-out mice to 15 μM of 22R-HC or 22S-HC. Mean ± s.e.m. of two pooled 15experiments. **, $P<0.01$; ***, $P<0.0001$ (Anova). **b**, Migration of CD11b+Gr1+ cells to 15 μM of 22R-HC or 22HS-HC following their pre-treatment with 500 ng of PTX or PTX control. Mean ± s.e.m. of two pooled experiments. *, $P<0.05$; **, $P<0.01$ (Anova). **c**, Migration of CD11b+Gr1+ cells towards 15 μM of 22R-HC, or 100 ng of CXCL5, SDF-1α or MIP-1α after pre-incubation (Pre) with 50 μM of 22R-HC. Mean ± s.e.m. of four pooled experiments. **, $P<0.01$; ***, $P<0.0005$ (Anova). **d**, Migration of CD11b+Gr1+ cells from WT, *Cxcr2*$^{+/-}$ and *Cxcr2*$^{-/-}$ mice to 15 μM of 22R-HC, or 100 ng CXCL5 and SDF-1α. Mean ± s.e.m. of four pooled experiments. **, $P<0.01$; ***, $P<0.0001$ (Anova). **e**, Flow cytometric analysis of CXCR2 expression by CD11b^{high}Gr1^{high} cells left untreated (UT) or incubated with SDF-1α, CXCL5, 22R-HC, 22S-HC or SB225002. Mean ± s.e.m. of three pooled experiments. **, $P<0.01$; ***, $P<0.0005$ (Anova). **f**, Effect of oxysterols and IL-8 on CXCR2-G protein coupling: 35S-GTPγS binding assay. Membrane aliquots from L1.2-CXCR2 cells were treated with the indicated concentrations of IL-8, 22R-HC or 22S-HC and the stimulation of 35S-GTPγS binding was evaluated. All data are expressed as percentage of basal 35S-GTPγS binding (set to 100%) and represent the mean ± s.e.m. of three experiments. **g**, Percentage of 125I-IL-8 bound to L1.2-CXCR2 cells in the presence of 100, 50, 10 or 1 μM of 22R-HC or 22S-HC. Mean ± s.e.m. of three pooled experiments. *, $P<0.05$ (Student's *t*-test). **h**, Percentage of WT and *Cxcr2*$^{-/-}$ CD11b+Ly6G+ neutrophils infiltrating RMA-Mock. Data are presented as mean ± s.e.m. of one experiment with six mice ($n = 6$). ***, $P=0.0003$ (Student's *t*-test).

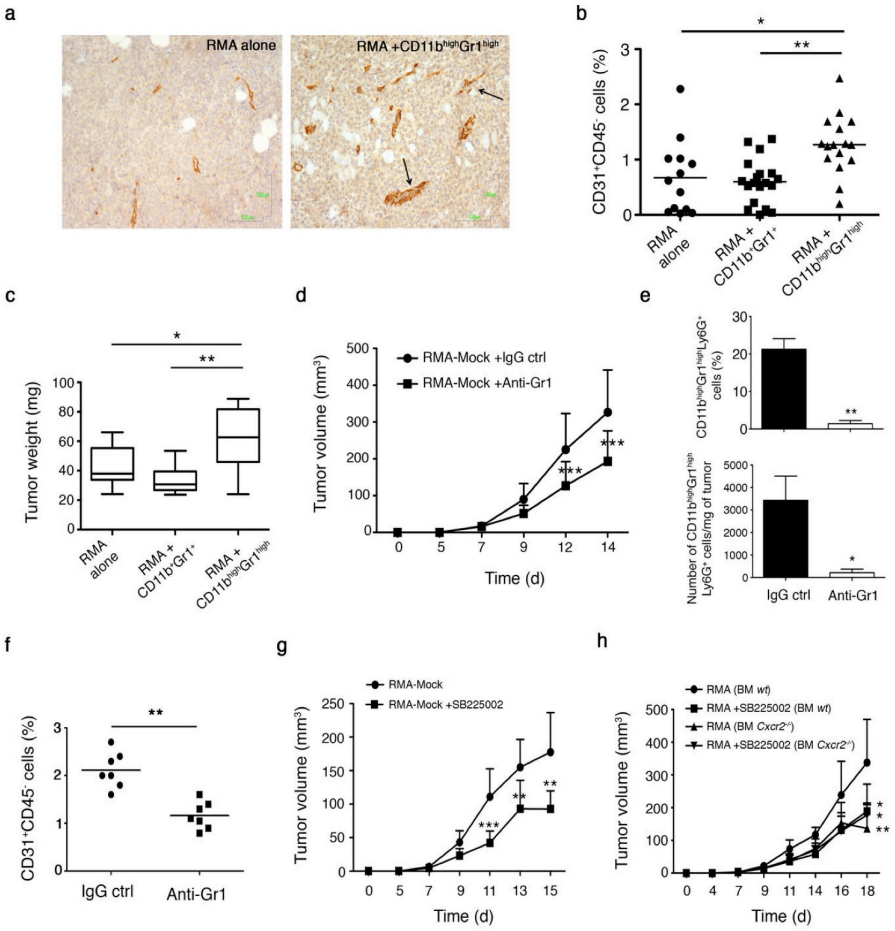
a
RMA alone
RMA +CD11b^high Gr1^high
b
CD31+CD45- cells (%)
RMA alone
RMA + CD11b+Gr1+
RMA + CD11b^high Gr1^high
c
Tumor weight (mg)
d
RMA-Mock +IgG ctrl
RMA-Mock +Anti-Gr1
Tumor volume (mm3)
Time (d)
e
CD11b^high Gr1^high Ly6G+ cells (%)
Number of CD11b^high Gr1^high Ly6G+ cells/mg of tumor
IgG ctrl
Anti-Gr1
f
CD31+CD45- cells (%)
IgG ctrl
Anti-Gr1
g
RMA-Mock
RMA-Mock +SB225002
Tumor volume (mm3)
Time (d)
h
RMA (BM wt)
RMA +SB225002 (BM wt)
RMA (BM Cxcr2-/-)
RMA +SB225002 (BM Cxcr2-/-)
Tumor volume (mm3)
Time (d)

Figure 4 | LXR ligand migrating neutrophils enhance tumour angiogenesis and growth. a, Immunohistochemistry showing CD31+ endothelial cells in RMA alone (left panel) or co-injected with $CD11b^{high}Gr1^{high}$ neutrophils (right panel). Arrows indicate enlarged and abnormally fenestrated vessels. Results of one out of four experiments. Scale bars, 100 µm. **b**, Percentage of CD45-CD31+ cells in RMA alone (*n* = 13) or co-injected with 22R-HC migrating (*n* = 16) or non-migrating cells (*n* = 19). Individual mouse data are shown (mean, horizontal line). *, *P*<0.05; ***, *P*<0.01 (Anova). **c**, Tumor weights of the experimental conditions as in **b**. *, *P*<0.05; ***, *P*<0.01 (Anova). **d**-**f**, Effects of intratumor neutrophil depletion. **d**, RMA tumor growth in mice administered intratumor with 30 µg of anti-Gr1 (*n* = 15) or control antibody (*n* = 15). ***, *P*=0.0001 (Anova). **e**, Percentage and number of RMA infiltrating neutrophils after intratumor administration of anti-Gr1 (*n* = 5) or control antibody (*n* = 5). *, *P*=0.038; **, *P*=0.0033 (Student's *t*-test). **f**, Percentage of CD45- CD31+ cells in RMA injected with anti-Gr1 (*n* = 7) or control antibody (*n* = 7). **, *P*=0.0031 (Student's *t*-test). **g**, Treatment of RMA-Mock-bearing mice with vehicle or 0.8 mM of CXCR2 antagonist SB225002. Mean ± s.e.m. of one experiment with 7-8 mice/group.**, *P*<0.001; ***, *P*=0.0009 (Anova). **h**, RMA growth in WT and *Cxcr2*$^{-/-}$ chimera mice, treated or not with 0.8 mM of SB225002. Mean ± s.e.m. of one experiment with 5-6 mice/group. *, *P*<0.05; **, *P*=0.0001 (Anova).

REFERENCES

1 Hanahan, D. and Weinberg, R. A., The hallmarks of cancer. *Cell* **100** (1), 57 (2000).

2 de Visser, K. E., Eichten, A., and Coussens, L. M., Paradoxical roles of the immune system during cancer development. *Nature reviews* **6** (1), 24 (2006).

3 Mantovani, A., Allavena, P., Sica, A., and Balkwill, F., Cancer-related inflammation. *Nature* **454** (7203), 436 (2008).

4 Zitvogel, L., Tesniere, A., and Kroemer, G., Cancer despite immunosurveillance: immunoselection and immunosubversion. *Nat Rev Immunol* **6** (10), 715 (2006).

5 Grivennikov, S. I., Greten, F. R., and Karin, M., Immunity, inflammation, and cancer. *Cell* **140** (6), 883.

6 Yang, L. et al., Expansion of myeloid immune suppressor Gr+CD11b+ cells in tumor-bearing host directly promotes tumor angiogenesis. *Cancer cell* **6** (4), 409 (2004).

7 Murdoch, C., Muthana, M., Coffelt, S. B., and Lewis, C. E., The role of myeloid cells in the promotion of tumour angiogenesis. *Nature reviews* **8** (8), 618 (2008).

8 Shojaei, F. et al., Role of myeloid cells in tumor angiogenesis and growth. *Trends Cell Biol* **18** (8), 372 (2008).

9 Nozawa, H., Chiu, C., and Hanahan, D., Infiltrating neutrophils mediate the initial angiogenic switch in a mouse model of multistage carcinogenesis. *Proceedings of the National Academy of Sciences of the United States of America* **103** (33), 12493 (2006).

10 Shojaei, F., Singh, M., Thompson, J. D., and Ferrara, N., Role of Bv8 in neutrophil-dependent angiogenesis in a transgenic model of cancer progression. *Proceedings of the National Academy of Sciences of the United States of America* **105** (7), 2640 (2008).

11 Fridlender, Z. G. et al., Polarization of tumor-associated neutrophil phenotype by TGF-beta: "N1" versus "N2" TAN. *Cancer cell* **16** (3), 183 (2009).

12 Repa, J. J. and Mangelsdorf, D. J., The role of orphan nuclear receptors in the regulation of cholesterol homeostasis. *Annu Rev Cell Dev Biol* **16**, 459 (2000).

13 Bensinger, S. J. and Tontonoz, P., Integration of metabolism and inflammation by lipid-activated nuclear receptors. *Nature* **454** (7203), 470 (2008).

14 Villablanca, E. J. et al., Tumor-mediated liver X receptor-alpha activation inhibits CC chemokine receptor-7 expression on dendritic cells and dampens antitumor responses. *Nature medicine* **16** (1), 98.

15 Fuda, H. et al., Oxysterols are substrates for cholesterol sulfotransferase. *J Lipid Res* **48** (6), 1343 (2007).

16 Wright, D. E. et al., Physiological migration of hematopoietic stem and progenitor cells. *Science (New York, N.Y* **294** (5548), 1933 (2001).

17 Pie, J. E. and Seillan, C., Oxysterols in cultured bovine aortic smooth muscle cells and in the monocyte-like cell line U937. *Lipids* **27** (4), 270 (1992).

18 Alberti, S. et al., Hepatic cholesterol metabolism and resistance to dietary cholesterol in LXRbeta-deficient mice. *J Clin Invest* **107** (5), 565 (2001).

19 Mantovani, A. et al., The chemokine system in cancer biology and therapy. *Cytokine & growth factor reviews* **21** (1), 27.

20 Yang, L. et al., Abrogation of TGF beta signaling in mammary carcinomas recruits Gr-1+CD11b+ myeloid cells that promote metastasis. *Cancer cell* **13** (1), 23 (2008).

21 White, J. R. et al., Identification of a potent, selective non-peptide CXCR2 antagonist that inhibits interleukin-8-induced neutrophil migration. *The Journal of biological chemistry* **273** (17), 10095 (1998).

22 Cacalano, G. et al., Neutrophil and B cell expansion in mice that lack the murine IL-8 receptor homolog. *Science (New York, N.Y* **265** (5172), 682 (1994).

23 Rajagopalan, L. and Rajarathnam, K., Structural basis of chemokine receptor function--a model for binding affinity

and ligand selectivity. *Bioscience reports* **26** (5), 325 (2006).

24 Joseph, P. R. et al., Probing the role of CXC motif in chemokine CXCL8 for high affinity binding and activation of CXCR1 and CXCR2 receptors. *The Journal of biological chemistry* **285** (38), 29262.

25 Wu, B. et al., Structures of the CXCR4 chemokine GPCR with small-molecule and cyclic peptide antagonists. *Science (New York, N.Y* **330** (6007), 1066.

26 Hogquist, K. A. et al., T cell receptor antagonist peptides induce positive selection. *Cell* **76** (1), 17 (1994).

27 De Santo, C. et al., Invariant NKT cells modulate the suppressive activity of IL-10-secreting neutrophils differentiated with serum amyloid A. *Nature immunology* **11** (11), 1039.

28 Shojaei, F. et al., Bv8 regulates myeloid-cell-dependent tumour angiogenesis. *Nature* **450** (7171), 825 (2007).

29 Strieter, R. M. et al., Cancer CXC chemokine networks and tumour angiogenesis. *Eur J Cancer* **42** (6), 768 (2006).

30 Vandercappellen, J., Van Damme, J., and Struyf, S., The role of CXC chemokines and their receptors in cancer. *Cancer letters* **267** (2), 226 (2008).

31 Shaked, Y. et al., Rapid chemotherapy-induced acute endothelial progenitor cell mobilization: implications for

antiangiogenic drugs as chemosensitizing agents. *Cancer cell* **14** (3), 263 (2008).

32 Hannedouche, S. et al., Oxysterols direct immune cell migration via EBI2. *Nature* **475** (7357), 524.

33 Liu, C. et al., Oxysterols direct B-cell migration through EBI2. *Nature* **475** (7357), 519.

34 Jensen, H. K. et al., Presence of intratumoral neutrophils is an independent prognostic factor in localized renal cell carcinoma. *J Clin Oncol* **27** (28), 4709 (2009).

35 Villablanca, E. J. et al., Selected natural and synthetic retinoids impair CCR7- and CXCR4-dependent cell migration in vitro and in vivo. *Journal of leukocyte biology* **84** (3), 871 (2008).

36 Sozzani, S. et al., Receptor expression and responsiveness of human dendritic cells to a defined set of CC and CXC chemokines. *J Immunol* **159** (4), 1993 (1997).

SUPPLEMENTARY METHODS

Purification of mouse neutrophils from the bone marrow. Neutrophils were purified from the bone marrow (BM) as described in1. Briefly, BM cells were flushed from femurs and tibias of C57Bl/6 6- to 8-wk-old mice using 4 ml of PBS (without Ca++ and Mg++). Cells centrifuged at 1200 rpm for 10 min were left for 30 sec in NaCl 0.2% to lyse red blood cells. Pooled BM eluates were then filtered through a 70-µm nylon cell strainer to remove cell clumps and bone particles and centrifuged at 1200 rpm for 10 min. The BM cell suspension was then carefully layered on top of a Percoll gradient (4 ml Percoll 80% + 4 ml Percoll 55%) and centrifuged at 2000 rpm for 30 sec at RT. The band located in between 55-80% was then collected, washed in PBS, counted and used for FACS analysis, migration experiments *in vitro* and *in vivo*, angiogenesis and binding assays.

Chemicals and reagents. Commercial chemicals were the purest available. Buthlyhydroxytoluene (BHT) and solvents of HPLC grade were obtained from Sigma-Aldrich (St. Louise, MO). The C18 cartridges (360 mg) were obtained from Waters Chromatography EUROPE (Netherlands). CXCL1 and CXCL5 ELISA kits were from R&D. Bv8 ELISA kit was from *Uscn* (Life Science inc.).

Sample collection for biochemical analyses. Tumor cells (RMA and NIH-3T3) were seeded at $1x10^5$ cells/ml and cultured for 48 hours. Then, conditioned media were collected, added

with buthylhydroxytoluene (40 μM final concentration) to avoid cholesterol oxidation2 and stored at -80° C until processing.

Solid-phase extraction of hydroxycholesterols. Hydroxycholesterol extraction was made as previously described. Briefly, the C18 cartridges were preconditioned with 1 ml of n-heptane/2-propanol (50:50, v/v), 1 ml of methanol and 2 ml of water. The cell free medium (2 ml) was then applied to the cartridge using only gravity. Afterwards, the cartridge was washed with 4 ml of methanol-water (75:25, v/v) and briefly dried under vacuum. Hydroxysterols were desorbed with 2 ml of n-heptane/2-propanol (50:50, v/v) using only gravity. The eluted substances were dried at 30°C by evaporation (Rotavapor; Büchi, Flawil, Switzerland), the residue was dissolved in 200 μl of methanol and subjected to CI-MS analysis and HPLC analysis.

Mass spectrometry analysis. Mass spectrometry was performed on a Thermo Electron TRACE DSQTM spectrometer through the rapid heating filament Direct-Exposure Probe (DEP) insertion mode. The mass spectrometric analyses were performed in chemical ionization (CI-MS) using methane as reactant gas at an electron energy of 70 eV with a source temperature of 200°C.

High performance liquid chromatography (HPLC). An HPLC method was developed based on the HPLC-ESI-MS methods described in4. Hydroxycholesterols were resolved using reverse phase HPLC (RP-HPLC) equipped with a Waters 996 Photoalide Array Detector (wavelength 213 nm). A 100 μl

aliquot of lipid extract (in methanol) or standard solution is loaded onto a RP-HPLC column (a 5 µm, 250 × 4mm LiChrospher 100 RP8 column, Merck) equipped with a guard column. Elution of hydroxycholesterols was carried out at flow rate of 300 µl/min, with a gradient formed by the solvent system A, consisting of methanol/water (85:15, v/v) and solvent system B consisting of methanol, both containing 5mM ammonium acetate. The gradient elution program was as follows: 3 min with solvent A; 33 min with a linear gradient from 100% solvent A to 100% solvent B; 15 min with 100% solvent B; 5 min with a linear gradient from 100% solvent B to 100% solvent A and maintained for 10 min to re-equilibrate the column prior to the next run.

Morphology of neutrophils. For the evaluation of the morphology of neutrophils, slides from LXR ligand migrating $CD11b^{high}Gr1^{high}$ cells were prepared by centrifugation at 1.500 rpm for 10 min in a Shandon Cytospin 3 (Shandon Lipshaw). Neutrophils were then stained using May-Grunwald-Giemsa. Cells were evaluated under light microscopy.

Real-Time RT-PCR and RT2 Profiler PCR Arrays experiments. Total RNA was isolated with TRIZOL (Invitrogen). Reverse transcription was performed from 1-2 µg of total RNA, using MLV-reverse transcriptase (Invitrogen). Quantitative PCR was performed using real-time PCR (ABI PRISM 7900, Applied Biosystems) using Sybr Green. The comparative Ct method was used to quantify transcripts normalized to cyclophillin as a gene reference. Primers for *Bv8*

have been reported in 5. Primers for *Cxcl5* are as follows: *Cxcl5* forward,GCTGCCCCTTCCTCAGTCAT;
reverse,CACCGTAGGGCACTGTGGAC.

RT2 Profiler PCR Arrays were performed using the Mouse Chemokines and Receptors RT2 ProfilerTM PCR Array (SABiosciences, Quiagen) according to manufacturer's instructions.

CXCL1 and CXCL5 ELISA assays. Seven day-established RMA-Mock and RMA- SULT2B1b tumors were collected and digested mechanically and enzymatically up to single cell suspension. Cells were counted and plated in 24 well plate (10^6 cells/well in 1 ml). After 24 hours supernatants were collected and the content of CXCL1 and CXCL5 was measured according to manufacturer's recommendations.

Bv8 ELISA assay. LXR migrating and non migrating cells plated in 24 well plate ($3x10^6$ cells/well in 1 ml) in the absence or in the presence of RMA-conditioned medium. After 24 hours supernatants were collected and the content of Bv8 was measured according to manufacturer's recommendations.

Tumor growth in *Lxr*$\alpha^{-/-}$ BM chimera. We transplanted lethally irradiated (11 Gy) C57BL/6 mice with BM from *Lxr*$\alpha^{-/-}$ or wt mice (5×10^6 BM cells per mouse). Eight weeks later, we carried out *Lxr*$\alpha^{-/-}$ genotype by PCR on blood cells, and used mice for tumor growth experiments.

OT-I proliferation assays. Splenocytes from OT-I mice were labelled with 4 μM CFSE (carboxyluorescein succinimidyl ester). Then they were washed and pulsed for 1 h at 37 °C with

SIINFEKL peptide (2 μg/ml). LXR ligand migrating and non-migrating CD11b+Gr1+ cells (1 x 10^5 or 5 x 10^4) were cultured in 96-well round- bottomed plates with 2 x 10^5 CFSE-labelled OT-I splenocytes. Cells were analyzed 4 days later with a FACSCalibur flow cytometer with FlowJo software. Data are presented as the percentage of proliferation of SIINFEKL-pulsed, CFSE-labelled OT-I splenocytes in the presence of LXR ligand migrating and non-migrating CD11b+Gr1+ cells relative to the proliferation of SIINFEKL-pulsed, CFSE-labelled- OT-I splenocytes alone (set as 100%). To test OT-I memory cells, we harvested OT-I splenocytes from OT-I mice previously immunized (ten days) with the SIINFEKL peptide (5 μg) emulsified in Complete Freund's Adjuvant.

Comparative Modeling. The human CXCR2 sequence was downloaded from the UniProt–Protein Knowledgebase database [entry P25025 (CXCR2)]. A model was built based on the human CXCR4 crystallographic structure (RCSB PDB ID: 3ODU). All the comparative modeling procedures were carried out with the Homology module of the Molecular Operating Environment 2010.10 (MOE). The alignment produced by the Align program of MOE with default parameters was manually edited according to T-COFFEE outputs. Comparative model building was carried out with the MOE Homology Model program. 3ODU was set as primary template. Ten independent models were built, and for each model 10 sidechain samplings at 300 K were performed. All the models were refined, then the highest scoring intermediate model was submitted to a further

round of energy minimization (EM). Both for the intermediate and the final structures the refinement procedures consisted in EM runs based on the AMBER99 force field, with the reaction field solvation model. The two- disulfide bonds, between cysteines 39 and 286, and between 119 and 196, were created by the MOE Builder module. The extracellular loops (ELs) were then submitted to energy minimization runs, after fixing TMs and ILs. Six EM runs, all down to an RMS gradient of 0.5 kcal/mol Å, were carried out while restraining the ELs atoms with a quadratic force from 105 down to 10-1 kcal/mol Å2. A further EM run was carried out without any restraint down to an RMS gradient of 0.5 kcal/mol Å. The quality of the final model was carefully checked with the MOE Protein Geometry module to make sure that the stereochemical quality of the proposed structure was acceptable.

Alignment between human CXCR2 and the selected crystallographic template human CXCR4 (3ODU)

```
3ODU             ------------------------------------PCFREENANFNKIFLPTIYSIIF
sp|P25025|CXCR2  MEDFNMESDSFEDFWKGEDLSNYSYSSTLPPFLLDAAPC-EPESLEINKYFVVIIYALVF

3ODU             LTGIVGNGLVILVMGYQKKLRSMTDKYRLHLSVADLLFVITLPFWAVDAVANWYFGNFLC
sp|P25025|CXCR2  LLSLLGNSLVMLVILYSRVGRSVTDVYLLNLALADLLFALTLPIWAASKVNGWIFGTFLC

3ODU             KAVHVIYTVNLYSSVWILAFISLDRYLAIVHATNSQRPRKLLAEKVVYVGVWIPALLLTI
sp|P25025|CXCR2  KVVSLLKEVNFYSGILLLACISVDRYLAIVHATRTLTQKRYLV-KFICLSIWGLSLLLAL

3ODU             PDFIFANVSEADD-RYICDRFYPNDL--WVVVFQFQHIMVGLILPGIVILSCYCIIISKL
sp|P25025|CXCR2  PVLLFRRTVYSSNVSPACYEDMGNNTANWRMLLRILPQSFGFIVPLLIMLFCYGFTLRTL

3ODU             SHSKGHQKRKALKTTVILILAFFACWLPYYIGISIDSFILLEIIKQGCEFENTVHKWISI
sp|P25025|CXCR2  FKAHMGQKHRAMRVIFAVVLIFLLCWLPYNLVLLADTLMRTQVIQETCERRNHIDRALDA

3ODU             TEALAFFHCCLNPILYAFLGAKFKTSAQHALTS----------------------------
sp|P25025|CXCR2  TEILGILHSCLNPLIYAFIGQKFRHGLLKILAIHGLISKDSLPKDSRPSFVGSSSGHTST

3ODU             --
sp|P25025|CXCR2  TL
```

Binding Site Analysis. The CXCR2 binding site was identified through the MOE Site Finder module, which uses a geometric approach to calculate possible binding sites in a receptor starting from its 3D atomic coordinates. This method is based not on energy models but on alpha spheres, which are a generalization of convex hulls[7].

Molecular Docking. The *in silico* molecular docking simulations were carried out with the Dock program contained in the MOE Simulation module. The full CXCR2 structure was set as Receptor. Before starting with the placement procedure, 1000 conformations were generated for each tested ligand by sampling its rotable bonds. The selected placement methodology was Triangle Matcher, in which the poses are generated by superposing triplets of ligand atoms and triplets of receptor site points. The receptor site points are alpha spheres centers that represent locations of tight packing. Before scoring all the generated poses, duplicate complexes were removed. Poses are considered as duplicates if the same set of ligand-receptor atom pairs are involved in hydrogen bond interactions and the same set of ligand atom::receptor residue pairs are involved in hydrophobic interactions. The accepted poses were scored according to the London dG scoring, which estimates the free energy of binding of the ligand from a given pose.

$$\Delta G = c + E_{flex} + \sum_{h-bonds} c_{HB} f_{HB} + \sum_{m-lig} c_M f_M + \sum_{atoms\_i} \Delta D_i \quad (1)$$

where *c* represents the average gain/loss of rotational and translational entropy; *Eflex* is the energy due to the loss of flexibility of the ligand (calculated from ligand topology only); *fHB* measures geometric imperfections of hydrogen bonds and takes a value in [0,1]; *c*HB is the energy of an ideal hydrogen bond; *f*M measures geometric imperfections of metal ligations and takes a value in [0,1]; *c*M is the energy of an ideal metal ligation; and *Di* is the desolvation energy of atom *i*. The difference in desolvation energies is calculated according to the formula:

$$\Delta D_i = c_i R_i^3 \left\{ \iiint_{u \notin A \cup B} |u|^{-6} \, du - \iiint_{u \notin B} |u|^{-6} \, du \right\} \qquad (2)$$

where *A* and *B* are the protein and/or ligand volumes with atom *i* belonging to volume *B*; *Ri* is the solvation radius of atom *i* (taken as the OPLS-AA van der Waals sigma parameter plus 0.5 Å); and *ci* is the desolvation coefficient of atom *i*. The coefficients {*c*, *cHB*, *cM*, *ci*} have been fitted from approx. 400 x-ray crystal structures of protein- ligand complexes with available experimental p*K*i data. Atoms are categorized into about a dozen atom types for the assignment of the *ci* coefficients. The triple integrals are approximated using Generalized Born integral formulas. Only the 300 top scoring solutions were kept and submitted to a further refinement step,

based on molecular mechanics (MM). In order to speed up the calculation, residues at a distance > 6 Å from the pre-refined pose were ignored, both during the refinement and in the final energy evaluation. All receptor atoms were held fixed during the refinement. During the course of the refinement, solvation effects were calculated using the reaction field functional form for the electrostatic energy term. The final energy was evaluated using the MMFF94x forcefield with the Generalized Born solvation model (GBIV)[8]. The estimated binding affinity and the ligand efficiency were calculated through the MOE LigX module. The *K*i was computed through the binding free energy estimated with the London dG scoring function.

REFERENCES

1 M. Corada, S. Chimenti, M. R. Cera et al., *Proceedings of the National Academy of Sciences of the United States of America* 102 (30), 10634 (2005).

2 F. Gilardi, B. Viviani, A. Galmozzi et al., *Neuroscience* 164 (2), 530 (2009). 3 I. Burkard, K. M. Rentsch, and A. von Eckardstein, *J Lipid Res* 45 (4), 776

(2004). 4 J. G. McDonald, B. M. Thompson, E. C. McCrum et al., *Methods in enzymology* 432, 145 (2007).

5 F. Shojaei, X. Wu, C. Zhong et al., *Nature* 450 (7171), 825 (2007).

6 C. Notredame, D. G. Higgins, and J. Heringa, *Journal of molecular biology* 302 (1), 205 (2000).

7 H. Eldesbrunner, M. Facello, R. Fu et al., *28th Hawaii International Conference on Systems Science* (1995).

8 M. Wojciechowski, T. Grycuk, J. M. Antosiewicz et al., *Biophysical journal* 84 (2 Pt 1), 750 (2003).

9 S. Vilar, J. Karpiak, and S. Costanzi, *Journal of computational chemistry* 31 (4), 707.

10 I. Eberini, A. G. Rocco, M. Mantegazza et al., *Journal of molecular graphics & modelling* 26 (6), 1004 (2008).

11 I. Eberini, P. Fantucci, A. G. Rocco et al., *Proteins* 65 (3), 555 (2006).

12 P. Ricchiuto, A. G. Rocco, E. Gianazza et al., *J Mol Recognit* 21 (5), 348 (2008).

Supplementary Table 1. Amino acids in CXCR2 binding site according to Site Finder classification.

N-term	CYS39	GLU40	PRO41	GLU42			
TM1	TYR55						
TM2	TRP104						
EL1	SER107	LYS108	TRP112				
TM3	SER123	LYS126	GLU127	PHE130	TYR131		
TM4	VAL180						
EL2	ARG184	SER189	VAL192	ALA195	CYS196	TYR197	GLU198
	ASP199	MET200	GLY201	ASN202	ASN203	TRP207	ARG208
TM5	LEU211	ARG212	PRO215				
TM6	TRP263	TYR266	LEU271				
EL3	ASP274	MET277	ARG278	GLN280	ILE282	GLN283	GLU284
	THR285	CYS286	ARG289	ASN290	ASP293	ARG294	
TM7	LEU296	ASP297	GLU300	ILE301			

Supplementary Table 1. Amino acids of the top-scoring binding site according to their potential hydrophobic contacts are reported. The CXCR2 binding site involves amino acids from different TMs and ELs, and several residues of EL2 seem to be crucial for the interaction. TM, Transmembrane; EL, Extracellular Loop.

Supplementary Table 2

Ligand	Docking energy (MM/GBIV)	pK_i
22(R)-HC	-16.4	9.49
7α-HC	-17.81	9.11
25-HC	-17.97	8.99
19-HC	-18.74	8.98
27-HC	-18.1	8.58
4β-HC	-15.4	8.52
22(S)-HC	-15.17	8.44
24-HC	-18.31	8.21

Supplementary Table 2. Molecular docking results between CXCR2 and 8 different oxysterols are reported. The top-scoring poses were selected through molecular mechanics with the generalized Born solvation model (MM/GBIV) energy score, since Vilar and colleagues[9] have suggested that this is the best choice for virtual screening in the absence of a training set. The reported p*K*i (-log dissociation constant) values are computed through the London dG scoring function. As already discussed by Eberini and

colleagues[10,11,12], this and other empirical scoring functions estimate the order of magnitude of the complex dissociation constant (rather than the dissociation constant proper). The different theoretical K*i* values measured for the 8 oxysterols range from approximately 0.3 to 6 nM (pKi from 9.49 to 8.21), suggesting that all these compounds are able to bind to CXCR2 binding site, and that 22R-HC has the most favorable theoretical pKi, which is directly connected to the binding free energy through the following relation: $\Delta G = -RT\ln(1/Ki)$, in which R is the gas constant and T is the absolute temperature.

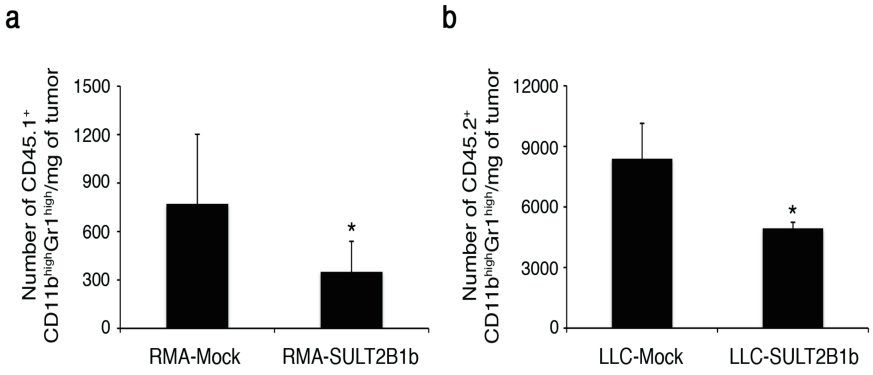

Supplementary Figure 1| a, Number of CD45.1+CD11b^{high}Gr1^{high} cells/mg of RMA-Mock or RMA-SULT2B1b tumors. Mean ± s.e.m of CD11b^{high}Gr1^{high} cells infiltrating RMA-Mock (n=12) and RMA-SULT2B1b (n=11) tumors. *, *P*<0.05 (Student's test). **b**, Number of CD45.2+ CD11b^{high}Gr1^{high} cells/mg of LLC-Mock or LLC-SULT2B1b tumors. Mean ± s.e.m of CD11b^{high}Gr1^{high} cells infiltrating LLC-Mock (n=3) or LLC-SULT2B1b (n=3) tumors. *, *P*<0.05 (Student's test).

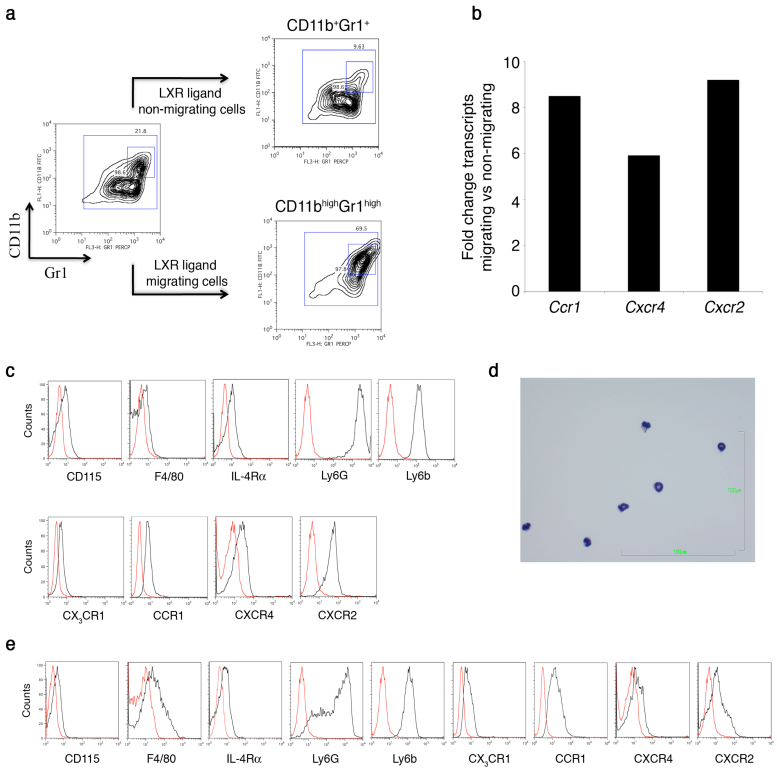

Supplementary Figure 2| Transcriptomic, phenotypic and morphologic analysis of LXR ligand migrating CD11b^{+}Gr1^{+} cells a, LXR ligand migrating cells are mainly CD11b^{high}Gr1^{high} cells, whereas non-migrating cells are CD11bGR1 cells expressing the two markers at intermediate levels. **b**, 22R-HC migrating CD11b^{high}Gr1^{high} cells express higher levels of mRNAs for Ccr1,Cxcr4 and Cxcr2 chemokine receptors than non-migrating CD11b^{+}Gr1^{+} cells. Mean ± experimental replicates from one representative experiment out of two performed by using the mouse chemokines and receptor RT^{2} Profiler PCR array. **c**, Flow cytometric analysis of 22R-HC migrating CD11b^{high}Gr1^{high} cells. They express high levels of CX_3CR1, CCR1,CXCR4 and CXCR2 chemokine receptors. Moreover, they express very high levels of the granulocytic/neutrophil markers Ly6G and Ly6b, whereas turn out to be negative or slightly positive for CD115 (M-CSF), F4/80 and IL-4Rα markers. One representative experiment is shown. **d**, Cytochemical analysis of 22R-HC migrating CD11b^{high}Gr1^{high} cells. The panel shows cells with lobulated and hypersegmentation or circular nuclei typical of mature and immature neutrophils. The slides were stained by May-Grunwald-Giemsa. Scale bars,100μm. **e,** Flow cytometric analysis of non-migrating CD11b^{+}Gr1^{+} cells. They express higher levels of F4/80 and CCR1 and lower levels of Ly6G and CXCR2 markes.

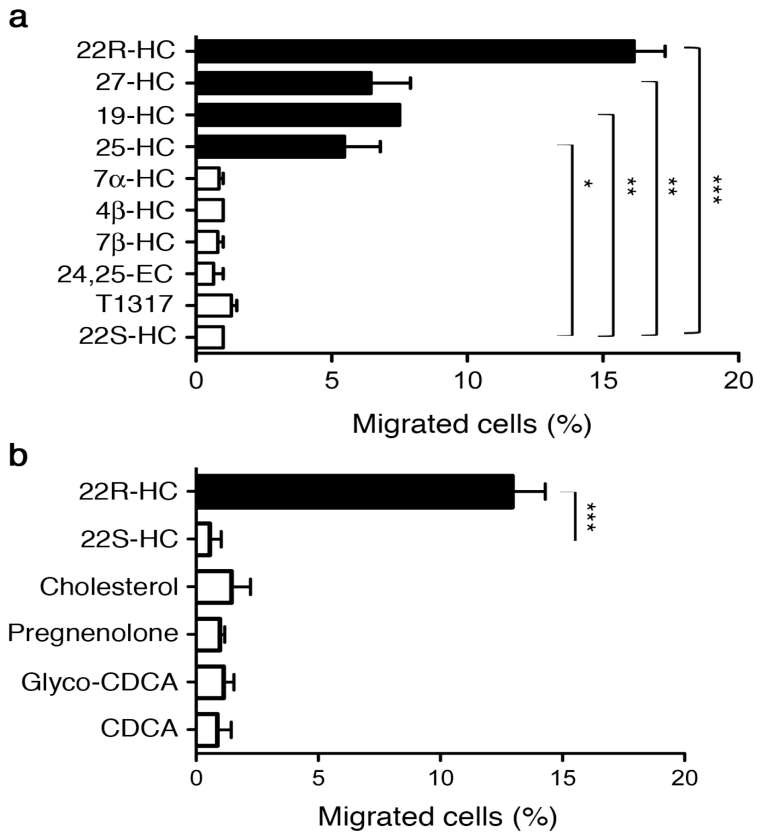

Supplementary Figure 3| Migration of purified CD11b^{+}Gr1^{+} cells to LXR ligands and to other sterol-derived compounds. a, 22R-HC, 22R-Hydroxycholesterol, 27-HC, 27-Hydroxycholesterol, 19-HC, 19-Hydroxycholesterol; 25-HC, 25-Hydroxycholesterol, 7α-HC, 7α-Hydroxycholesterol; 4B-HC,4B-Hydroxycholesterol; 7B–OH, 7B–Hydroxycholesterol; 24,25 EpoxyChol cholesterol; T1317,T0901317;22S-HC Hydroxycholesterol. All ligands except 7α-HC, 24,25-EC and 19-HC were tested at 15μM. Due to toxicity, α-HC, 24,25-EC were tested at 5μM, whereas 19-HC at 1μM. Mean ± s.e.m of two pooled experiments (n=2). *, *P*<0.05; ** , P<0.01, *** , P<0.0001 (Anova). **b,** CDCA, Chenodeoxycholin Acid; GlycoCDCA, Glycine Chenodeoxycholin Acid. CDCA and GlycoCDCA are FXR ligands, Pregnenolone is a SXR ligand. Mean ± s.e.m of three pooled experiments (n=3). *** , P<0.0001 (Anova).

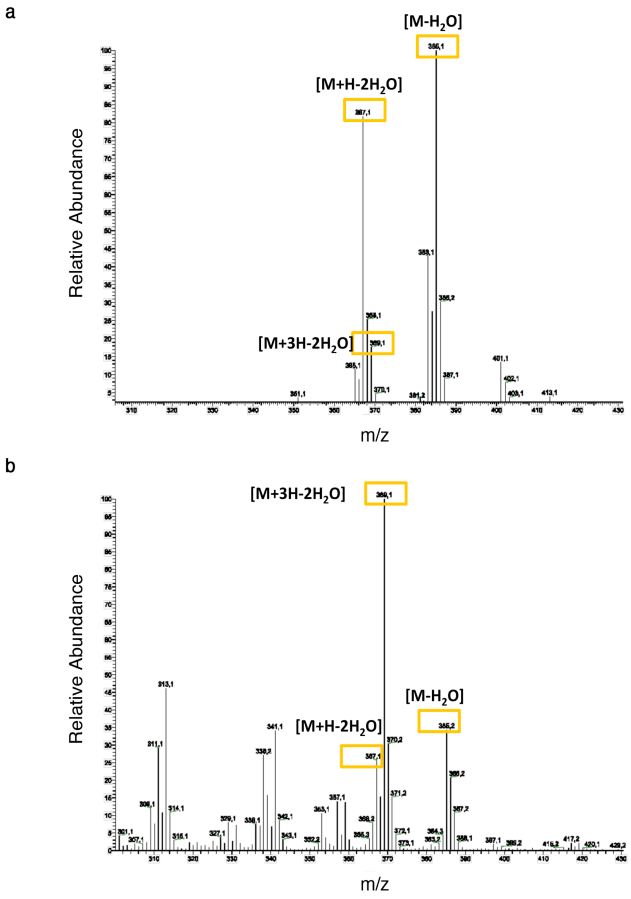

Supplementary Figure 4| Chemical Ionization-Mass Spectrometry analysis. a, The spectrum derived from 1mM hydroxyxholesterol mix solution (containing 22R,22S,25,27,19,7α and 4B-HC) is shown. The molecular weight for all hydroxycholesterol used is 402.67 kDa. The collision product ion pathway was constituted by the followed fragment ions: m/z 385 (M-H2O), m/z 367 (M+H-2H20) and m/z 369 (M+3H-2H20). **b**, Spectra derived from RMA hydroxycholesterols extract. The same molecular ions m/z 385,m/z 369 and m/z 367, as in **a** are detected.

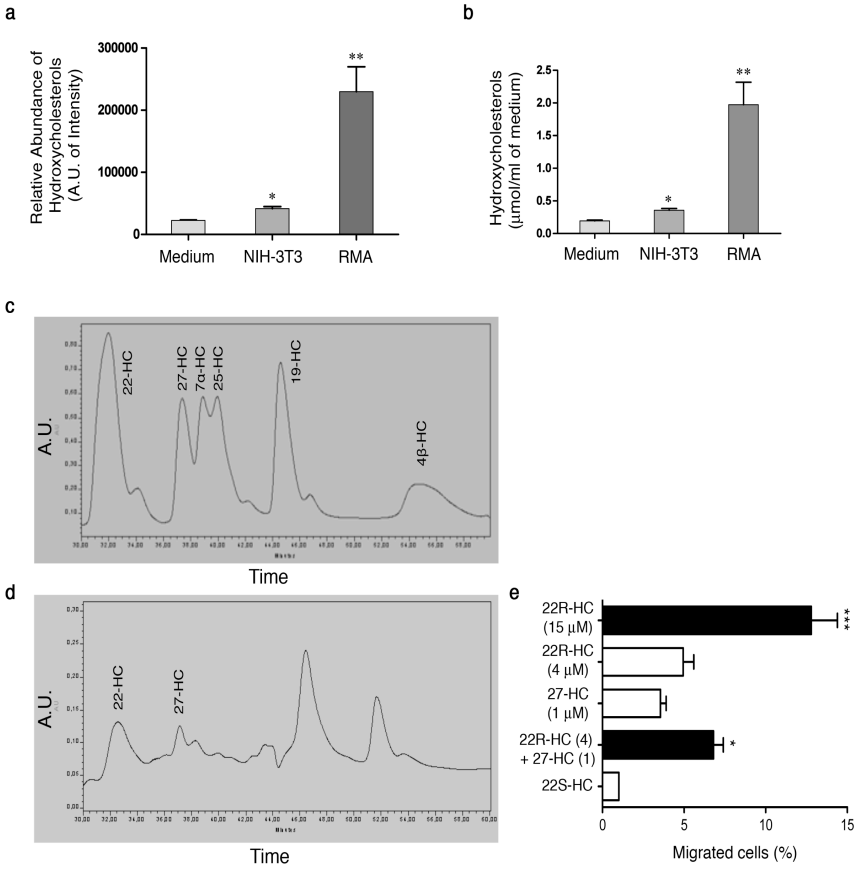

Supplementary Figure 5| Quantification of Hydroxycholesterol in cell supernatants and HPLC analysis. a, The relative abundance of the 3 major fragmentation ions (m/z 385, m/z 369 and m/z 367) is expressed as arbitrary intensity units (A.U.) with respect to 1mM mix solution of hydroxycholesterols. **b**, The concentration of hydroxycholesterol with respect of ml off media (μmol/ml) is reported. The results are expressed as Mean ± s.e.m values of three different experiments (n=3).). *, *P*<0.05 versus Medium values;). **, *P*<0.01 versus NIH-3T3 conditioned medium (anova). **c-d,** HPLC chromatograms of 7 single hydroxycholesterol standard (**c**) and of hydroxycholesterol extract from RMA conditioned medium (**d**). Two main hydroxycholesterol are identified on the basis of the retention time: the 22-HC and 27-HC in a ratio of 4:1. **e**, The mix of the two oxysterols in a ratio of 4 to 1 is able to induce a statistically significant migration of $CD11b^{high}Gr1^{high}$ cells. as Mean ± s.e.m of two pooled experiments (n=2). *, *P*<0.05, ***, P<0,0001 (Anova).

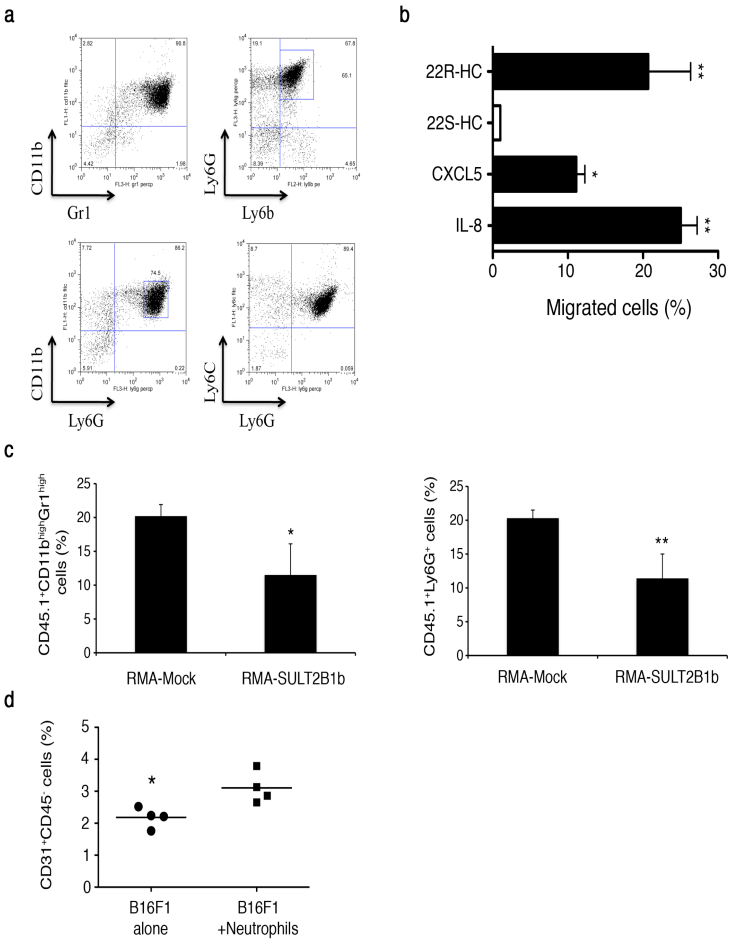

Supplementary Figure 6| In *vitro* and in *vivo* assays of neutrophils isolated from bone marrow by standard methods. a, FACS analysis of *bona fide* neutrophils isolated by percoll gradients from bone marrow. They express CD11b, GR1 and Ly6G and Ly6b markers. One representativ experiment out of four pooled experiments (n=4). *, *P*<0.05, ** , P<0,01 (Anova). **c**, Percentages of CD45.1+CD11b^{high}Gr1^{high} or CD45.1+Ly6G+ neutrophils infiltrating RMA-Mock or RMA-SULT2B1b are shown as mean ± s.e.m (n=3 mice). * P=0,034, ** P=0,020 (Student's *t*-test). **d**,Percentage of CD45^{-}CD31^{+} cells in B16F1 alone (n=4) or co-injected with BM purified neutrophils (n=4). Individual mouse data are shown (mean, horizontal line). *, *P*<0.05 (Student's *t*-test).

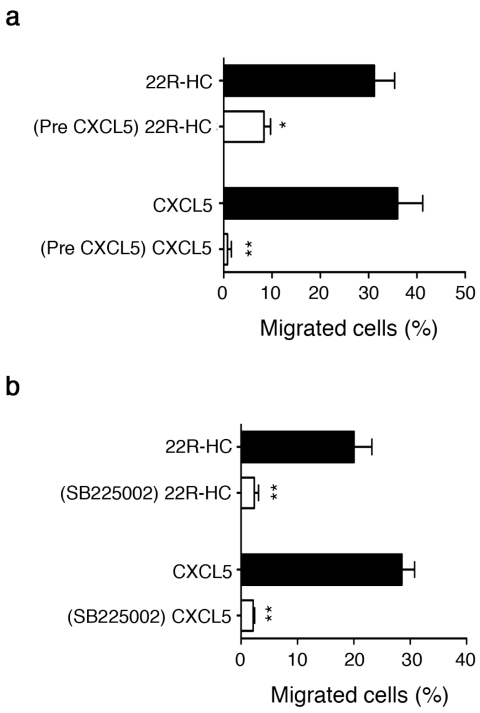

Supplementary Figure 7| Desensitizaion experiments. a-b, Migration of neutrophils (*i.e*, $CD11b^{+}Gr1^{+}$ cells) towards 22R-HC or CXCL5, after pre-incubation (Pre) with CXCL5 (**a**) or with the CXCR2 antagonist SB225002 (**b**). Mean ± s.e.m of two pooled experiments (n=2). *, *P*<0.05, ** P<0,01 (Anova).

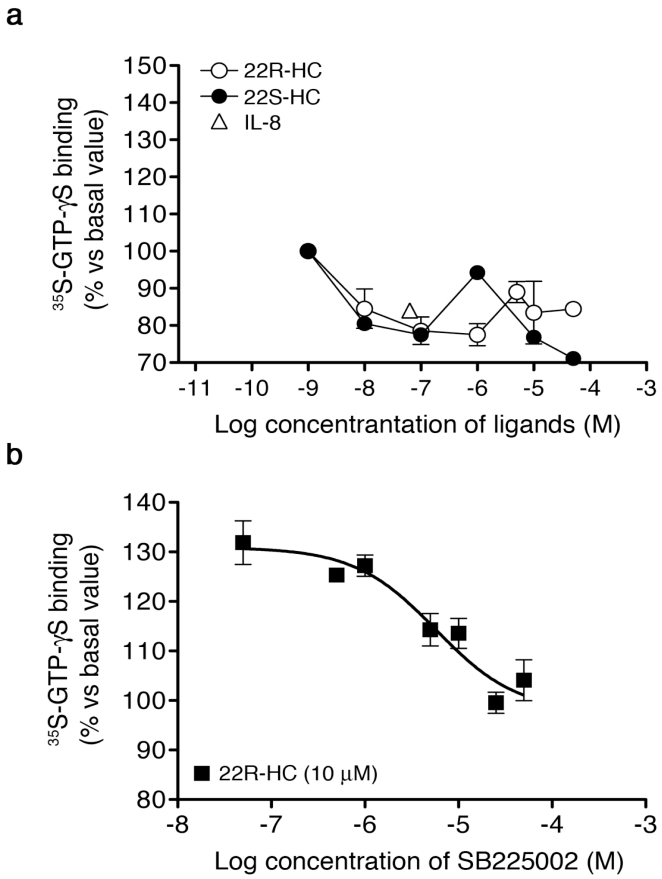

Supplementary Figure 8| Pharmacological characterization of oxysterols as ligand for CXCR2. a, Characterization of oxysterols as agonists for CXCR2. Various concentrations of 22R-HC, 22S-HC oxysterols or the natural CXCR2 ligand IL-8 were used to stimulate ^{35}S-GTP-S incorporation in Mock-L1.2 cell membranes. All data are expressed as percentage of basal ^{35}S-GTPS binding (set to 100%) and represent the mean ± s.e.m of 3 different experiments each performed in duplicate. **b**, Dose dependent inhibition of ^{35}S-GTPS incorporation in CXCR2-L1.2 cell membranes treated with 22R-HC (10 μM) and increasing amounts of the CXCR2 antagonist SB225002. IC_{50} is 14,63 μM. All data are expressed as percentage of basal ^{35}S-GTPS binding (set to 100%) and represent the mean ± s.e.m of 3 different experiments.

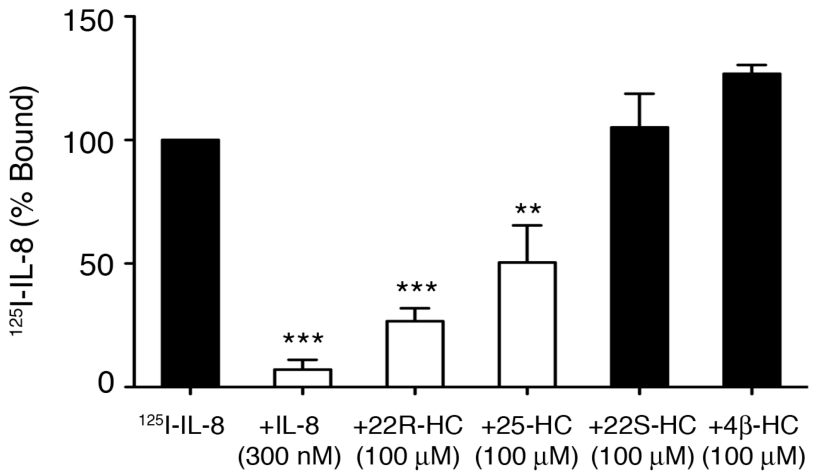

Supplementary Figure 9| Binding assays with different of oxysterols. Percentage of ^{125}I-IL-8 bound to L1.2-CXCR2 cells, alone or in the presence of 300 nM of IL-8, 100 μM or 22R-HC, 25-HC, 22S-HC or 4β-HC.
We observed the displacement of radioactive IL-8 when L1.2 cells expressing mCXCR2 were incubated with 100 μM of 22R-HC (74,5% inhibition) and 25-HC (50% inhibition), but not with 22S-HC or 4β-HC. Mean ± s.e.m of five pooled experiments. **, *P*<0.01, ***, P<0,0001 (Anova).

a

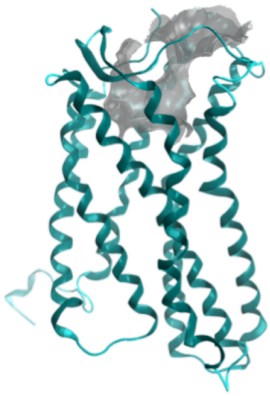

b

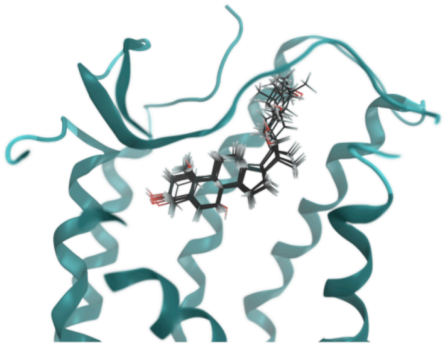

Supplementary Figure 10| Models of interaction between CXCR2 and oxysterols. a, Yhe analysis of CXCR2 by the MOE Site Finder module revealed 8 putative binding sites; the top-scoring one contained 401 potential contact atoms, among which 58 were hydrophobic and 284 involved side chain atoms. This site is localized in an extracellular region inside the ELs and close to the plasma membrane (binding site II, according to [23,24]). **b**, The superposition of the top-scoring poses for all the tested ligands shows a common binding fashion, involving the same set of residues in the binding site. The differences in the pKi values for the tested oxysterols may be connected with the variable position of the hydroxyl functionated to the arrangement of the aliphatic chain connected to C17 in the cyclopentane ring.

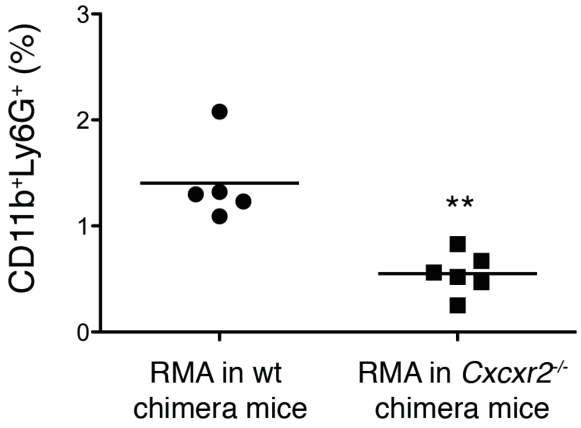

Supplementary Figure 11| Percentage of $CD11b^{+}Ly6G^{+}$ neutrophils infiltrating RMA-Mock tumors (16 days after tumor infusion) injected in wide-type bone marrow chimera (n=5) or in $CXCR2^{-/-}$ (n=6) bone marrow chimera mice. **, *P*<0.0010 (Student's *t*-test).

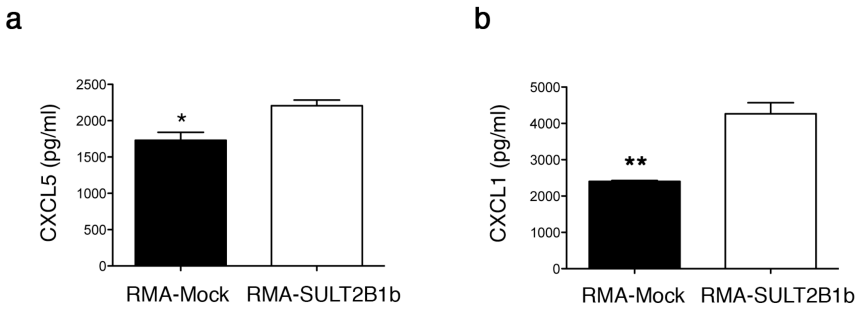

Supplementary Figure 12| CXCL5 and CXCL1 production by cell suspensions isolated from RMA-Mock and RMA-SULT2B1b tumors.
a-b, Cell suspensions from RMA-SULT2B1b tumors release higher amounts of CXCL5 (**a**) and CXCL1 (**b**) chemokines than cell suspensions from RMA-Mock. Cell suspensions isolated from tumors established for 7 days were collected and analyzed by ELISA. Results are from three pooled experiments. *, *P*<0.05, **, P<0,01 (Student's *t*-test).

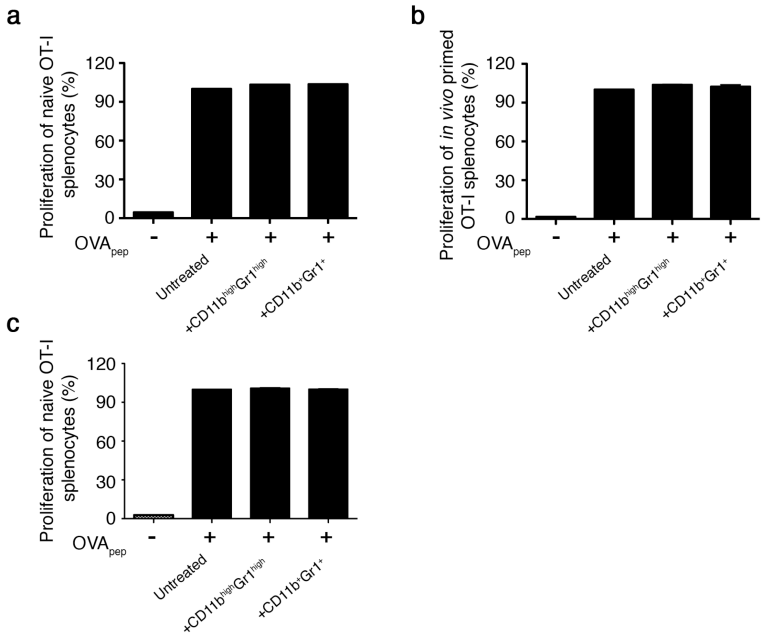

Supplementary Figure 13| 22R-HC migrating neutrophils do not suppress OVA-specific T cells. a-b, Proliferation of OT-I splenocytes naive (**a**) or memory (**b**) labelled with cytosolic dye CFSE and pulsed with the ovalbumin peptide SIINFEKL in the presence of 50% $CD11b^{high}Gr1^{high}$ or $CD11b^{+}Gr1^{+}$ cells. Mean ± s.e.m of experimental replicates from one representative experiment out of two. **c**, Proliferation of OT-I splenocytes naive labelled with the cytosolic dye CFSE and pulsed with the ovalbumin peptide SIINFEKL in the presence of 50% $CD11b^{high}Gr1^{high}$ or $CD11b^{+}Gr1^{+}$ cells, isolated from RMA-bearing mice (established for 19 days). Mean ± s.e.m of experimental replicates from one representative experiment out of two.

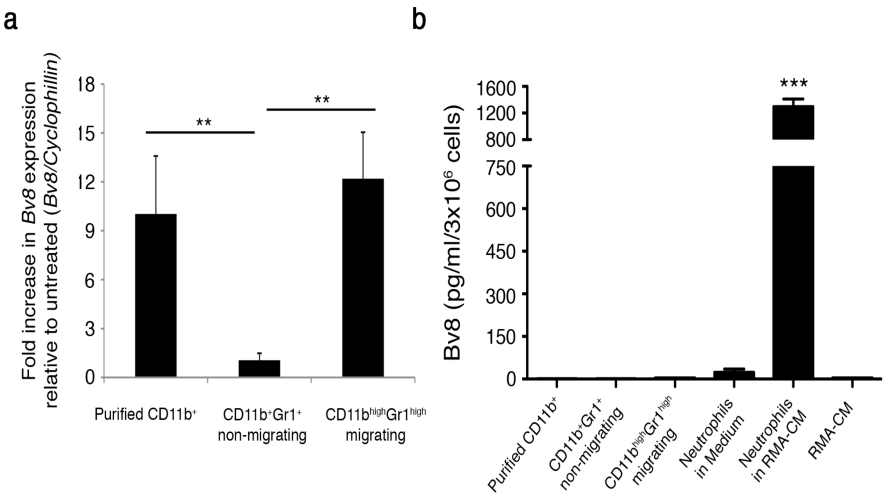

Supplementary Figure 14| Bv8 production by CD11b^{high} Gr1^{high} neutrophils. a, qPCR for Bv8 mRNA in purified CD11b^{+}, 22R-HC migrating and non-migrating cells. Mean ± s.e.m of three pooled experiments. **, *P*<0.01 (Anova). **b**, Release of Bv8 protein by purified CD11b^{+}, 22R-HC migrating and non migrating cells and by purified neutrophils incubated overnight with medium or RMA-Conditioned Medium (RMA-CM), and by RMA-Conditioned Medium (RMA-CM). Bv8 is mainly released by neutrophils incubated with RMA-CM. Neutrophils incubated with Medium release neglectable amount of Bv8. Mean ± s.e.m of three pooled experiments. *** , P<0,0001 (Anova).

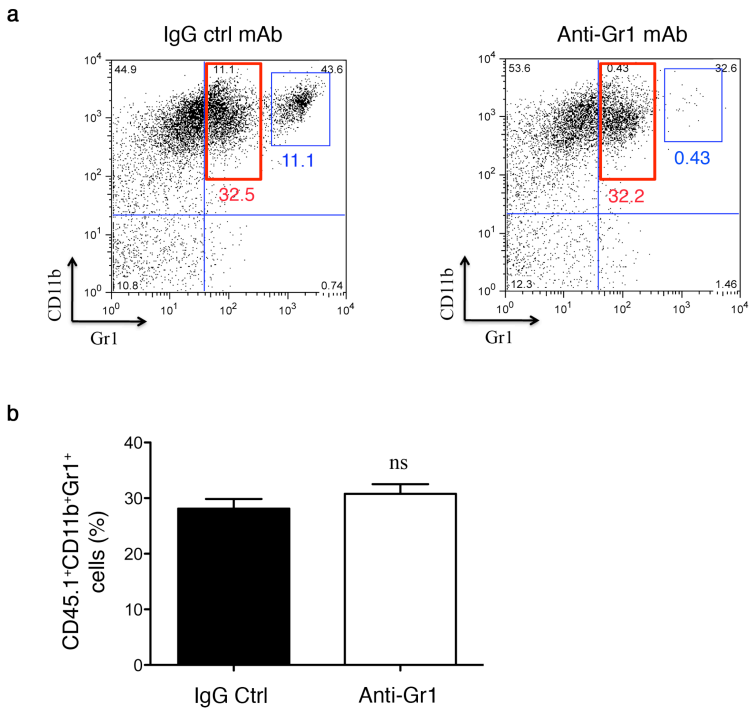

Supplementary Figure 15| Intratumor treatment with the anti-Gr1 mAb depletes only CD11b^{high}Gr1^{high} cells. FACS analysis showing specific deletion of CD11b^{high}Gr1^{high} cells when mice are treated intratumor with anti-Gr1 (1A8) mAb. CD11bGr1 cells expressing the two markers at intermediate level are unaffected by the treatment. One representative experiment is shown. **b**, Percentages of CD11b^{+}Gr1^{+} (expressing CD11b and Gr1 at intermediate levels) infiltrating RMA-Mock treated with IgG ctrl mAb (n=5 mice) or treated with anti-Gr1 (1°8) mAb (n=5 mice) are shown as Mean ± s.e.m ns, not significant (Student's *t*-test).

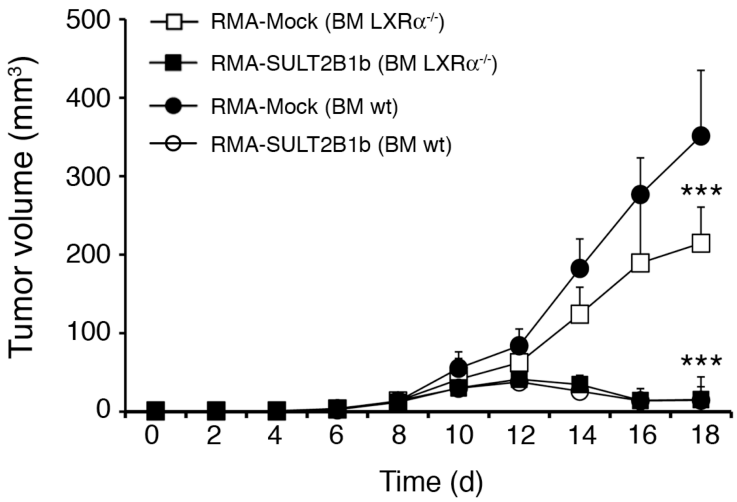

Supplementary Figure 16| Growth of RMA-Mock and RMA-SULT2B1b in Lxrα$^{-/-}$ or wilde-type (wt) chimeras. The inactivation of LXR ligands achieved by the enzymatic activity of SULT2B1b is more effective than the abrogation of LXRα signaling in promoting tumor rejection. Mean ± s.e.m of one experiment with 9-10 mice/group. ***, *P*<0.0001 (Anova).

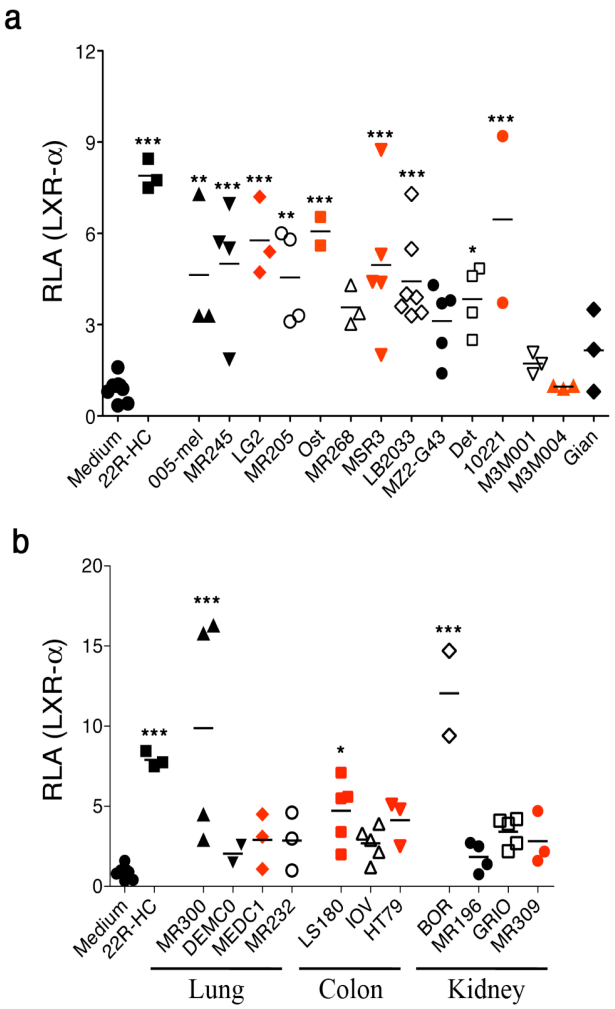

Supplementary Figure 17| Human tumours release LXR ligands (a,b). Conditioned medium from human melanomas (**a**), lung, colon and kidney (**b**) tumours were collected and tested for the presence of LXR ligands by luciferase-based reporter assay. *, $P<0.05$ **, $P<0.01$, ***, $P<0.0001$ (Anova). Each symbol corresponds to one tumor-conditioned medium tested and the line represents the mean value. RLA, Relative Luciferase Activity.

Chapter 3

CONCLUSIONS AND FUTURE PERSPECTIVES

Cancer cells are able to counteract immune system recognition and destruction in a process defined as immune evasion. Indeed, tumors release immune suppressing molecules and/or metabolites, such as amino acids, glycoproteins and lipids, actively altering tumor microenvironment and, therefore, dampening the ability of immune cells to destroy tumor cells[1,2,3,4]. On the other hand, recruited immune cells may promote tumor progression by producing cytokines or angiogenic factors[5]. It has been shown that MDSCs can accumulate into tumors and in part differentiate to macrophages. Neutrophils unlike macrophages are released into the blood as mature or nearly mature cells, but like macrophages can exist in different states of activation, depending on signals present within the microenvironment. Indeed, pro-inflammatory neutrophils are able to recruit T cells to the tumor site[6]. Conversely, pro-tumor neutrophils can induce neoangiogenesis or inhibit T cells proliferation. It has been demonstrated that mouse and human tumors can release chemokines attracting neutrophils within the tumor. As an example, CXCL1 and CXCL5 attract neutrophils in a CXCR2 depend-manner.

We previously identified oxysterols as molecules capable of

inhibiting the chemokine receptor CCR7 expression on maturating DCs, through the activation of the nuclear receptor LXRα[7]. The down-regulation of CCR7 impairs the migration of dendritic cells to secondary lymphoid organs, hence dampening antitumor immune responses. We also demonstrated that the inactivation of LXR ligands by SULT2B1b was more effective in controlling tumor growth as compared to LXR deficiency.

In the first part of this work, we demonstrated that tumor releasing LXR ligands are involved in the recruitment of $CD11b^{high}Gr1^{high}$ neutrophils into tumors. Indeed, we found an increased number of $CD11b^{high}Gr1^{high}$ cells infiltrating the lymphoma RMA (RMA-Mock) as compared to the same tumor expressing the SULT2B1b (RMA-SULT2B1b). This effect was related to tumor-derived oxysterols because both tumors released the CXCL5 and CXCL1 chemokines. Our results also showed that among the well-known oxysterols only a few of them (22R-HC, 27-HC, 25-HC and 19-HC) could induce $CD11b^{high}Gr1^{high}$ migration, even if at different extent. Moreover, the migration of these cells was specific for oxysterols and not for other sterol-derived nuclear receptor ligands (*i.e.*, primary bile acids, pregnenolone, etc.). This suggests that both the affinity and chemical structure of oxysterols are important for neutrophil migration. Notably, we excluded the involvement of LXR receptors in neutrophils migration because LXR$\alpha/\beta^{-/-}$ cells migrated to oxysterols similarly to what observed for wild-type cells. By desensitization assays, we demonstrated that oxysterols induced neutrophil migration by engaging the

CXCR2 receptor. Accordingly, we observed that 22R-HC down-modulated the expression of CXCR2 on neutrophils and inhibited the binding of the radioligand ^{125}I-IL-8. The formal demonstration that CXCR2 receptor was involved in the 22R-HC-mediated neutrophil migration was established using CXCR2 knock out mice for *in vitro* and *in vivo* experiments. *In vitro*, we did not detect any migration of *Cxcr2*$^{-/-}$ neutrophils towards 22R-HC. *In vivo*, when we injected a mixed of CD11b^{high}Gr1^{high} cells (from wild type and *Cxcr2*$^{-/-}$ mice) in RMA-bearing mice, we found mainly wild type neutrophils infiltrating the tumors.

In the second part of this work, we investigated the role of oxysterol-migrating neutrophils in tumor growth. Previous studies have shown the ability of tumor-infiltrating neutrophils to augment neoangiogenesis and tumor growth by releasing pro-angiogenic factors and matrix-degrading enzymes[8]. Here, we demonstrate that neutrophils migrating to 22R-HC have a higher level of *Bv8* mRNA as compared to non-migrating cells and are able to actively release Bv8 when are conditioned by the supernatant of RMA tumor. The angiogenic effect of 22R-HC-migrating neutrophils was demonstrated by angiogenesis assays, based on the co-injection of neutrophils and tumor cells in mice. Indeed, we found a higher percentage of CD31^{+} endothelial cells than in control tumors. Moreover, these tumors grew faster than controls.

The relevance of neutrophils in this setting was demonstrated by experiments of intratumor neutrophil depletion, in which we

observed a delay of tumor growth. The role of CXCR2 was evaluated in CXCR2 knock-out bone marrow chimera mice, where we observed a delay of tumor growth. In conclusion, the results reported here indicate that oxysterols can recruit tumor-promoting immune cells in an LXR-independent manner by binding the CXCR2 chemokine receptor. The $CD11b^{high}Gr1^{high}$ recruited neutrophils promote in turn neoangiogenesis and tumor growth.

In near future, we will investigate the role of neutrophils in other tumor models, *i.e.* spontaneous tumor models investigating the molecular pathways leading to the local production and release of oxysterols during tumor formation and progression. Moreover, we will characterize the molecular mechanisms blunting the antitumor features of neutrophils in favor of their acquisition of pro-tumor ability.

REFERENCES

1 Fallarino F., Grohmann U., You S., McGrath B. C., Cavener D. R., Vacca C., Orabona C., Bianchi R., Belladonna M. L., Volpi C., Santamaria P., Fioretti M. C., Puccetti P. (2006) The combined effects of tryptophan starvation and tryptophan catabolites down-regulate T cell receptor ζ-chain and induce a regulatory phenotype in naive T cells. J. Immunol. 176, 6752–6761.

2 Greenhough A, Smartt HJ, Moore AE et al (2009). The COX-2/PGE2 pathway: key roles in the hallmarks of cancer and adaptation to the tumour microenvironment. Carcinogenesis 30:377–386.

3 Uyttenhove C., Pilotte L., Theate I., Stroobant V., Colau D., Parmentier N., Boon T., Van den Eynde B. J. (2003) Evidence for a tumoral immune resistance mechanism based on tryptophan degradation by indoleamine 2,3-dioxygenase. Nat. Med. 9, 1269–1274.

4 Grohmann U., Bronte V. (2010) Control of immune response by amino acid metabolism. Immunol. Rev. 236, 243–264

5 A. Mantovani, S. Sozzani, M. Locati, P. Allavena, A. Sica (2002) Macrophage polarization: tumor-associated

macrophages as a paradigm for polarized M2 mononuclear phagocytes Trends in immunology 11,549-555

6 Fridlender, Z.G. et al. Polarization of tumor-associated neutrophil phenotype by TGF-β: “N1” versus “N2” TAN. Cancer Cell 16, 183–194 (2009).

7 Villablanca, E. J. et al., Tumor-mediated liver X receptor-alpha activation inhibits CC chemokine receptor-7 expression on dendritic cells and dampens antitumor responses. Nature medicine 16 (1), 98.

8 Shojaei, F., Singh, M., Thompson, J. D., and Ferrara, N., Role of Bv8 in neutrophil-dependent angiogenesis in a transgenic model of cancer progression. *Proceedings of the National Academy of Sciences of the United States of America* **105** (7), 2640 (2008).

RINGRAZIAMENTI

Desidero ringraziare il Dr. Vincenzo Russo per avermi seguito con inesauribile e infinita pazienza in questi anni, che vanno oltre i tre anni di dottorato. Vorrei ringranziarlo, per avermi dato la possibilità di crescere scientificamente, confrontarmi e persistere nel fare questo affascinante lavoro, che è la base della conoscenza dell' esistere di ogni uomo. Lo ringrazio anche per avermi sopportato, nei momenti altalenanti della mia vita, che come sempre dico, è fatta di alti e bassi. Vorrei ringraziare anche tutte le persone che hanno lavorato con me, Raffaella, Dani e Andrea Leiva. Ringrazio tantissimo anche la dott.ssa Catia Traversari, per i suoi preziosi consigli e il Dr. Silvano Sozzani, per la sua immensa disponibilità, competenza e per i suoi consigli riguardo il far ricerca. Con maggiore enfasi vorrei ringraziare le mie amiche (per forza) CLAUDIA LANTY, CELESTE AIDA, AURORA e il mio amico, anche lui per forza, ANDREA alias SPOKKIO JUNIOR. Vorrei ringraziarli perché ogni tanto ma non sempre hanno understood i miei momenti down o meglio di solitudine; li ringrazio anche perché ormai mi capiscono anche quando parlo in un'altra lingua che non è né l'italiano ne' l'inglese comunque l'importante è che io mi sono capita. Ovviamente ,vorrei ringraziare con grandissimo amore, i miei genitori, i miei fratelli e i miei amici, non per forza Gero, Pamela, Samanta, Ilenia, Edoardo, Francesco e Cesare che sono sempre al mio fianco. Come ultimo, ma non con meno valore, vorrei ringraziare il mio Oscuro PostDoc Matias alias SPOKKIO SENIOR e la sua allieva Marta, insieme alla sua amica candeggina Noemi che con la loro simpatia e vivacità mi hanno fatto star molto bene in questi ultimi mesi. Ringrazio tutti, anche coloro che ho escluso, dicendo che alla fine, come tutte le cose, il lavoro fatto fino adesso verrà lasciato ai posteri e d' ora in poi si ricomincia, con una nuova meta. Ongoing life … pensavate ad experiments ?!!!